IDENTIFYING PERMEABILITY CONTROLS BY USE OF GRAVITY METHOD IN MENENGAI GEOTHERMAL FIELD, KENYA

JOSEPH MUTHII GICHIRA

A Thesis report presented for Award of Master of Science Degree in Geothermal Technology, in Geothermal Training and Research Institute, Dedan Kimathi University of Technology.

May 2018.

STUDENTS' DECLARATION

This thesis is an original work presented only in this University/institution for consideration and certification.

Signature…….

Date…….

Muthii Gichira

G296-03-013/2013

Declaration by Supervisors:

I can confidently report that this project was done by the candidate under my supervision as the approved supervisor.

Professor Nicholas Mariita

Institution: ……..

Signature 

Date…..

Doctor Antony Wamalwa

Institution: ……..

Signature…….....

Date…..

DEDICATION

This research is dedicated to my wife for her continued support throughout the study period.

ACKNOWLEDGEMENT

I would wish to give thanks to Geothermal Development Company who is my employer for accepting my request to take this Master of Science course at Dedan Kimathi University. Many thanks to the Director of Geothermal Training Institute, Professor Nicholas Mariita for his encouragement to the students whenever we showed signs of giving up and his role as my supervisor. Special mention to my other supervisor, Doctor Antony Wamalwa for his dedication to ensure I come out of this course with complete understanding of my subject of interest. To Doctor Jean Bosco Byiringiro, your advice on research methods and design of experiments was immeasurable and for that I say, thank you. To the entire Dedan Kimathi University family for the time we spent together during those weekends, thank you. To my wife, thank you so much for being there for me even when I couldn't find enough time to spend with you.

ABSTRACT

Surface studies done in Menengai field have indicated a huge geothermal potential and has led to the drilling of several wells. However, some of these wells have not produced as earlier projected and there are questions as to whether this field has enough permeability. The purpose of this study was to employ gravity method to understand density variations in the Menengai field by developing structural models and establishing whether there is enough permeability. Raw data received from Kengen and GDC was reduced to simple Bouguer data by subjecting it to all reduction procedures and gravity models developed using a Golden software program called Surfer. These models were then subjected to specific filters that helped in identification of structures responsible for permeability. These filters are: Band pass filter; applied to remove certain wavelengths, horizontal derivative filter; applied to image zones of sharp contrasts. Density inversion from results of simple Bouguer anomaly readings were generated by 3D inversion Grablox1.6 programme that calculated synthetic gravity anomaly of a 3D block model. Comparison of gravity and resistivity models indicates a good resemblance of the magmatic intrusion and the Tecto-Volcanic Axis (TVA's). From this analysis, permeability controls for Menengai geothermal field were identified as follows: caldera rim faults that contribute mostly to deep vertical recharge, NNE-SSW faults along Solai graben, NNW-SSE faults along Molo axis, the southern fault extending towards Lake Nakuru and the uplifting dome in the central part of the caldera which enhance further fracturing within the caldera. This has led to a conclusion that there is enough permeability in Menengai geothermal field. The research and its findings therefore have shown that gravity should be used as a key technique rather than a preliminary tool in geothermal exploration. The practice has mainly been to use gravity for deformation monitoring or as a preliminary tool. However, failure by other techniques in identifying permeability controls forms the basis of this study and from the results; it has been found that if well utilised gravity method could solve the many challenges encountered in geothermal exploration. The results from this study therefore would be of high importance to GDC if adopted and used in locating sites where geothermal wells can be drilled and to future researchers.

TABLE OF CONTENTS

LIST OF FIGURES

LIST OF TABLES

ABBREVIATIONS AND ACRONYMS

TVA - Tectono Volcanic Axis.

NNW - North North West orientation/direction.

NNE - North North East orientation/direction.

NW - North West orientation.

NW-SE - North West to South East orientation.

NE-SW - North East to South West orientation.

N-S – North to South orientation.

GDC - Geothermal Development Company.

Kengen - Kenya Electricity Generating Company.

MWe - Mega Watts electricity.

EM- Electromagnetics

TEM - Transient electromagnetic.

MT - Magneto tellurics.

MW-01 A- Menengai well one A.

Ma - Million years.

c.g.s - Centimetre gram second system of units.

SI- International System of Units

CHAPTER ONE

1. INTRODUCTION

1.1 Introduction

Chapter one highlights the area where the study was carried out giving a background of the study area. It introduces the area as a geothermal field and shows its location within the Kenyan section of the Rift. The chapter also focuses on the tectonic setting of the rift since this has a direct relationship with the topic of study. Also covered is the surface and structural geology for their significance on permeability. In summary, this chapter has covered the location and geology of the area.

1.2 Background of the study

Menengai is a field with huge geothermal potential. The field stands in an area of intra-continental crustal three-way rift intersection with the main Rift meeting the Nyanzian Rift. The main Rift is confined by North - South running rift scarps. The field covers the Ol-Banita plains towards northeast, Solai graben, Ol'Rongai and Menengai volcanoes.

This study paid more attention on the Menengai Volcano. This portion of the rift represent a splinter segment of the main lithospheric units as supported by high-pitched slopes on the flank to the east while on the west is a moderately inclined one (Bosworth, Lambiase, & Keisler, 1986). The central loop assemblies of Olbanita and Menengai calderas characterise failures related to withdrawal near surface magma compartments beneath. From an extract obtained from a report by Burke & Dewey, 1973, it was explained that there could be a mantle plume superimposed by Menengai – Ol'banita zone. The surface was said to include numerous eruptive volcanoes with caldera failures and concentration

of tectonic grid faulting - block and fissure faults in its northern extents typical of extensional faulting related to divergence at crustal boundaries.

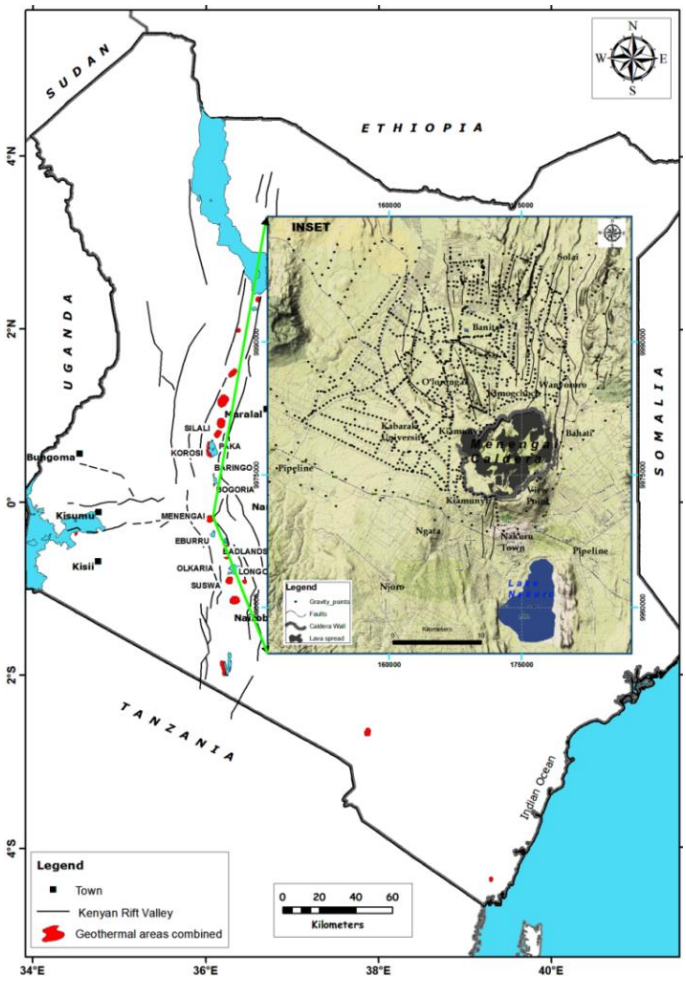

Figure 1: The Kenya Rift section showing position of Menengai(Omenda, 2007).

Massive volumes of pyroclastics shelter the gradients of Menengai and Ol'banita areas. These differ from welded pyroclastic flows, pumice rich ash deposits, ash fall and nearby lithic tuff projections adjacent to Menengai caldera. The source of these pyroclastics eruptives is the violent eruption leading to development of Menengai caldera (Simiyu et al., 2001).

Geophysical investigations forms a key part since they are the only approach of detecting abysmal structures responsible for controlling the geothermal system which includes heat sources and conduits for geothermal fluids, with the latter being the missing link in many areas and hence a let-down in geothermal development. Gravity technique is very powerful in this regard but much attention has always been directed towards resistivity and seismic methods and even when used most workers tend to concentrate mainly on identifying heat sources. Kenya map displaying the position where Menengai lies within the Kenya Rift Valley, Figure 1. A detailed geology account of this area is given in this section under subsections 1.2, 1.3 and 1.4.

1.3 Tectonic setting

The Kenya Rift section is a prominent geographical and geological feature of interest. It is a tectonic feature running north to south. It forms a typical graben averaging 40 to 80 km wide, see Figure 1. The Kenyan section of the Rift is a portion of the great African Rift system which is an intra-continental separation region where rift tectonism accompanied by intense volcanism, has taken place from late Tertiary to Recent. The rift developed in an unchanging orogenic belt that abuts around a craton. Numerous Quaternary volcanoes occur within the Kenyan segment of the Rift floor. Within the rift floor, majority of the volcanic centres had single or multiple explosive phases which included collapsing of calderas. Several centres have scattered hydrothermal expressions and are imagined to accommodate geothermal systems driven by magmatic sources.

The Menengai field is situated in a zone associated with complex tectonic activity connected three way rift intersection. This section of the split is characterised by divergence forces with east -west pulls occasioned block faulting, comprising of sloping

slabs as manifested in the two scarps plus the rift floor. The western region is characterised with narrow scarps that have been eroded resulting in gentle scarps, an indication of slight effects of movements. On the other hand, the eastern margins portray broader loops, with high-pitched slopes suggesting immediate dynamic activities.

There seems to be constant extension tectonics beneath the floor of the rift channel as demonstrated by several normal faults traversing this channel. Two TVA's essential in controlling Menengai geothermal system are: Molo TVA and Solai TVA.

1.4 Surface Geology

Figure 2 is a simple geology map of the Menengai area. The areas around the caldera are concealed by pyroclastics which erupted from centres related with Menengai volcano. The main caldera is in filled with post caldera lava flows which are young in age. Regions to the north exhibit Trachytic and phonolitic Pleistocene lavas superimposed by the main Menengai volcanics. Alluvials are found in low lying narrow grabens where they are placed as thin layers.

Menengai area is divided into three distinct regions whose external rocks paint different eruption styles for simplicity of explanations, these are: northern region comprising of escarpments with exposed older lava flows, the central region consisting of level grounds enclosed by by-products of plinian explosions with limited interfering escarpments and the Menengai. The caldera floor is filled largely by post caldera eruptives. The post caldera eruption lavas are believed to have followed volatile periods manifested by tuffaceous materials present in the caldera.

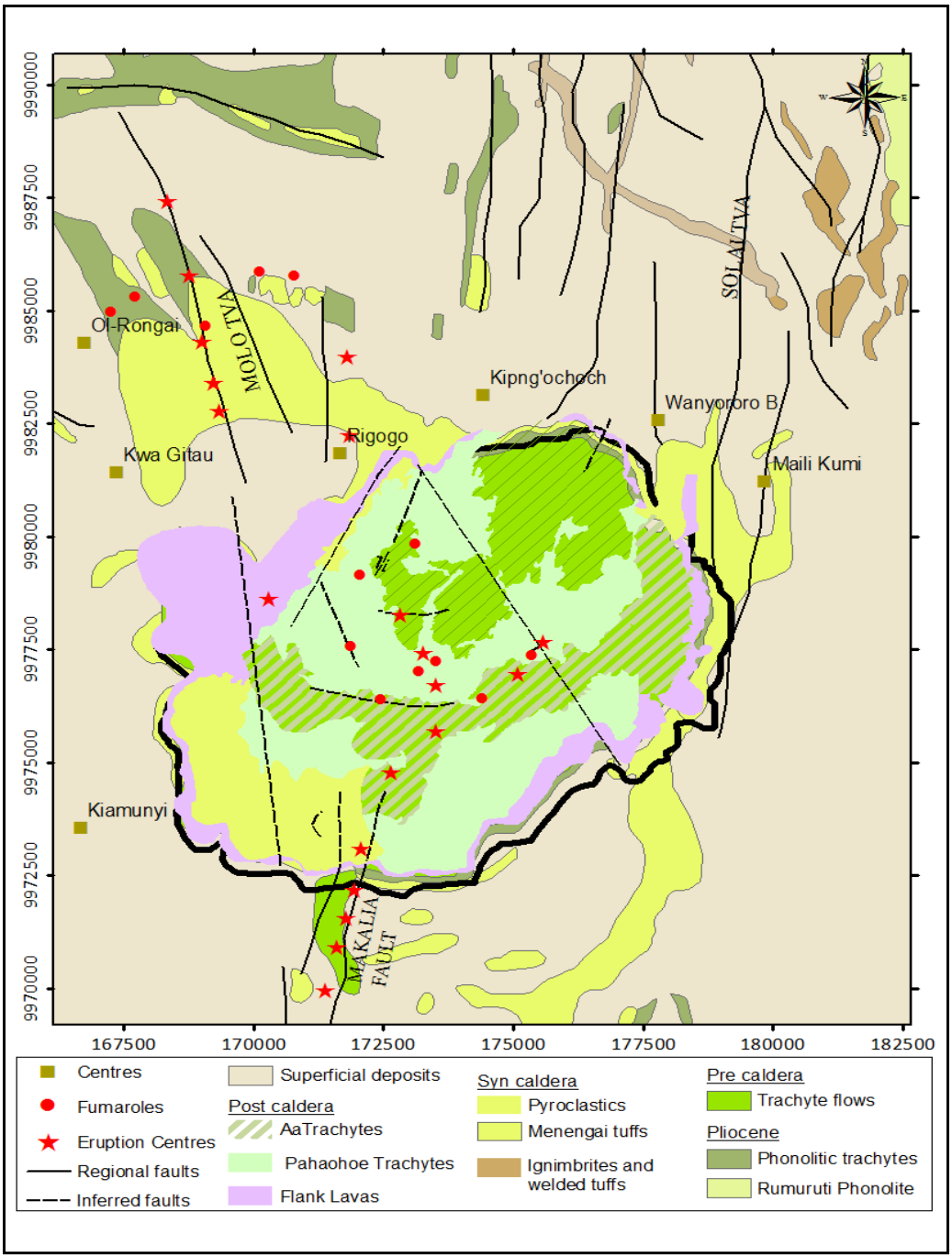

Figure 2: Geology of Menengai map. (Modified from Robinson, 2015)

1.5 Structural Geology

The regional tectonics map examines the structural systems of the wider Menengai area, Figure 3. The main systems in this region are classified into three categories, namely:

Menengai caldera, Molo TVA and Solai TVA. The groups are independently discussed herein.

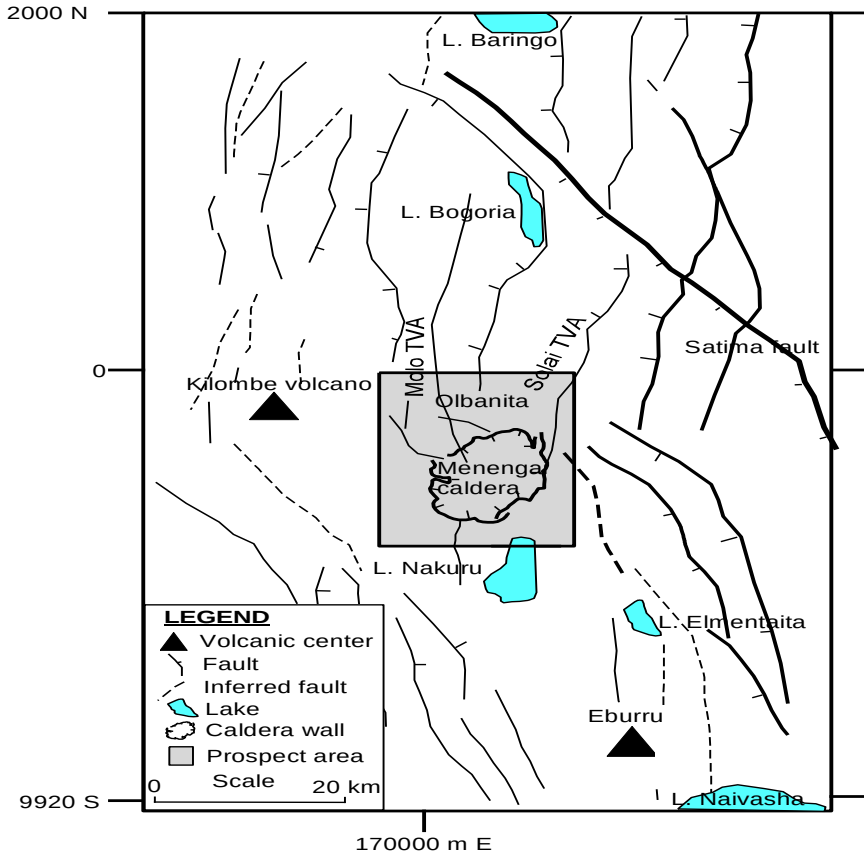

Figure 3: Structural map of Kenya. (Mungania et al., 2004)

1.5.1 Menengai Caldera

This large cauldron-like depression forms an oval sunken landform that has a main axes stretching for 11.5 kilometres and a minor axes estimated to measure 7.5 kilometres. The disk shaped caldera rim fault is effectively conserved with the sloping gradient measuring around 400 metres at selected places. The loop structure is disturbed on the NE end by the Solai graben faults and to SSW of the caldera wall by a fracture extending southwards, Figure 3. Notable disturbances are also evident in the NW and SE ends and could be pre caldera grabens. The floor of the caldera is covered by after caldera lavas to the level that

it is impossible to approximate collapse depth and structures inside the caldera floor. On the other hand, the caldera floor is covered by lavas from fissure eruptions.

1.5.2 Molo Tectono-volcanic Axis

Molo TVA is a notable physical feature symbolized externally by a region characterised with faults and breaks through which eruptions take place (Geotermica Italiana, 1987), Figure 3. The feature stretches from south eastern part of Lake Baringo basin and areas to the east of Lake Bogoria where it creates a 4 km graben cutting through Lake Bogoria phonolites a distant up north of the study region. On the eastern limits of Molo TVA are the Arus steam jets. This structure also advances to the south below Menengai volcanics and re-emerges again in the Ol'rongai region.

The Ol'rongai system forms part of the greater Molo TVA that has been characterised by numerous volcanic activities before such as eruptions that occasioned the formation of a NNW drifting continuous elevated crest.

1.5.3 Solai Tectono-volcanic Axis

This axis forms a graben that is 4 km in width trending in a north-south orientation extending from the east of the caldera and past Solai. The axis comprises several N- S trending faults structures. The eastern edge of the graben perhaps spreads to the base of Marmanet scarp. The northern end passes via L. Bogoria trachy-phonolites, north west of Kisanana. The southern extension beneath the Menengai volcanic load is an important hydrogeological control and likely permeability improvement of fragile lava formations underlying the Menengai eruptives.

1.6 Problem Statement

After many years of using geophysical methods in geothermal exploration in Kenya, little is known of permeability before drilling. Information on permeability before drilling is a must have for increased confidence and assured success. This has been a major challenge and if not well dealt with could act as an impediment to the country's set target of electricity from geothermal resources.

1.7 Objectives

This study was guided by the following main and specific objectives.

1.7.1 Main objective

The main intention for this research was to carry out gravity data modelling to understand density variations in the Menengai caldera and therefore uncover the subsurface structures with more focus on the fracture zones.

1.7.2 Specific Objectives

The specific goals of this research were:

i. To develop gravity structural models.
ii. To establish the presence of permeability.
iii. To compare Gravity models with Resistivity models.

1.8 Research Questions

This research sought to answer these three questions:

i. Can gravity method be successfully used in determining permeability?
ii. Is there permeability in Menengai?
iii. Is there a relationship between gravity models and existing resistivity models?

1.1 Significance of the Study

Gravity method is good in identifying subsurface structures; however previous works concentrated mainly on identifying the heat sources or intrusions. For a complete geothermal system, three main components are important, namely: heat source, permeability and a cap rock; out of the three, permeability is the most elusive.

1.2 Limitations of the Study

This research work was undertaken within the Kenyan Rift Valley which is characterised by numerous fault structures. The limitation to this study therefore is that its findings might not be used as a template or a guide in sedimentary environment.

1.3 Assumptions of the Study

This study assumed that gravity method is good for identifying buried structures and therefore best for characterising permeability.

CHAPTER TWO

2. LITERATURE REVIEW

2.1 Introduction

Geothermal is a term used to refer to energy confined in the rocks and fluids filling fractures and pores in rocks within the earth's crust. The key source of geothermal energy is understood to be radioactive decay happening deep inside the earth (Smith, 1983). This chapter looks into detail the current geothermal trends in Kenya i.e. a short history from 1950's to date and the MWe realised so far. The chapter covers a short overview of permeability since this forms the basis of this study. Also discussed herein are the different geothermal exploration techniques namely: geology, geochemistry and geophysics. Theory and application of gravity method used as a tool for identification of permeable areas is also discussed in this chapter. Review of previous works done is covered in detail and deductions made revealing gaps that needed further study.

2.2 Geothermal Development in Kenya

Geothermal exploration in Kenya has been on-going ever since the fifties and so far, the country has an estimated geothermal potential of 10,000 MWe (Gichira 2012) yet only 676.8 MWe has been realised and connected to the grid. This is approximately 30 per cent of the total installed capacity. Much of this comes from Olkaria geothermal field with an installed capacity of 674.4 MWe and a pilot plant in Eburru geothermal field producing the remaining 2.4 MWe. Further expansion of geothermal has been accelerated by commissioning of 335 MWe in 2014-2016 from conventional power plants and well head units. Production drilling at the Olkaria geothermal project for an extra 560 MWe plants to be established under the on-going Public Private Partnership arrangement between the

private sector and Kengen. Currently, Geothermal Development Company is drilling in Menengai field with an aim of realizing 105 MWe scheduled for commissioning sometime in 2018. Areas where detailed surface data has been acquired includes: Korosi, Baringo, Silali, Paka, Longonot and Suswa with exploration drilling anticipated to begin soon in Silali and Baringo.

2.3 Permeability

The ability of rocks to transmit fluids through the pore spaces is called permeability, it is denoted by k and its SI unit is m^2 (Schön 2015). This is dependent on the connectivity of pore spaces, thus permeability is interrelated to porosity. Pore spaces need to be interlinked and packed with water for fluid transmission to take place (Heap et al., 2018). The extent of pore interconnectivity is called effective porosity. The variation of permeability values in geological materials is enormously big with the most permeable materials having values that are many times higher than the least permeable ones. In addition to the features of the host material, fluid pressure and viscosity also influence the flow speed of fluids (Lee et al., 2006)

2.4 Different exploration disciplines

Geothermal energy exploration involves different disciplines namely; geophysics, geochemistry and geology. Under geophysics, there are different techniques which include: magnetics, gravity, seismology and electromagnetism.

2.4.1 Geophysics

The science that involves study of physical parameters of the earth e.g. magnetism, density, seismicity and resistivity of rocks is referred as geophysics (Lowrie 1997).

In geothermal resource surveys, gravity and magnetic investigations are employed mostly for mapping geological structures. The main applications are identifying the location and depth of buried intrusives, locating faults and dikes and the depth to the basement. In particular, magnetic method is useful in evaluating paleo-magnetism and locating hydrothermally-altered areas while gravity on the other hand is employed to map geological formations and density contrasts. Subsurface rocks have different densities, thus diverse gravitational forces.

Seismic measurements can be either active or passive. Active seismic involves mounting of sensors at different strategic positions in the ground followed by injection of waves into the ground. The energy that reflects back at different times and locations on the surface is then recorded using geophone receivers. When this data is processed, information about the subsurface, including the types of rocks and fault structures is extracted. This information can also be compared with gravity to get more precise velocity models which offer better depth approximations, hence, beneficial while developing conceptual models and ultimately finding drilling locations.

A passive seismic method involves mounting of sensors at strategic positions in the area of interest and makes use of micro-earthquake activities which are induced naturally. When this data is retrieved and processed, it is then used to outline permeable fractures that forms flow conduits for geothermal fluids and demarcate the fragile-tensile zone. This information could also be useful in monitoring important pointers in induced and natural reservoir phase changes during geothermal resource exploitation (Simiyu & Keller, 1998).

Electromagnetic methods have been confirmed to be beneficial geophysical tools in exploration of geothermal resources. This is because spatial distribution of conductivity in geothermal areas is determined by the host rock distribution and is also directly related to

the distribution of the real exploration goal (Berktold, 1983). Two main methods are employed here namely Transient electromagnetic (TEM) and Magnetotellurics (MT).

2.4.2 Geochemistry

The use of tools and principles of chemistry to describe the mechanisms behind key geological systems such as the Earth's crust and oceans is referred to as geochemistry (Sentosa 2018). Geochemical techniques are an important and a useful addition to the hydrological, geological and geophysical techniques employed in geothermal energy development. Geochemical techniques are applied from the exploration stage to the plant operation stage of geothermal energy development.

The chemistry of thermal fluids collected at the surface is used as an indicator of fluid behaviour in the subsurface. Geochemical study of thermal fluids provides information on the origin, temperature, flow pattern and other characteristics of the subsurface fluids. Chemical reaction within thermal fluids is controlled by equilibration of chemical components in the fluids according to changes in temperature, boiling, variation in host rocks and other changes in physical conditions.

2.4.3 Geology

The role of geology in geothermal exploration is mainly for search of heat source and permeability. Geological mapping of the surface geology is used as proxy to the condition of the source of heat. In Menengai the caldera pyroclastics have dated and this has been discussed by several scientists. A number of these researchers and their important findings are given here, i.e. Jones and Lippard (1979) said the post-caldera is1400 years old. (Leat 1983) explained that the younger lavas are 12,850 years while the older lavas were dated to 29,000±300 years. Later (Geotermica Italiana, 1987) based its research on carbon dating of paleo-soils and approximated the age of the eruptives to be 14,900±900 years.

Similar lava flows of equivalent freshness (lacking disturbances) like the Olkaria's Ololbutot lavas are dated around 180±50 years (Clarke, et al., 1986). This young age of the rocks in volcanoes is an important indicator of an active magma system hence heat source.

Geological structures are in important for fluid paths and are good targets for well drilling. Menengai surface data indicate that most important structures are N-S and NW-SE. These are related to regional tectonics. A result from current drilled wells proves this fact, e.g. well MW-01A encounters a NW-SE resulting in a very productive well. Geological structures are mapped using remote sensing and by traverses in the field.

Findings from these three disciplines; geophysics, geochemistry and geology are incorporated to develop conceptual models for successful geothermal resources development. For successful exploration, development and utilization of geothermal resources, a clear definition and knowledge of attributes related to the area of concern is essential. To achieve this, a conceptual model which is an expressive and qualitative model incorporating the essential physical features of the system is developed.

2.5 Gravity Method

2.5.1 Theory

This method is centred on two Newton's laws: the Law of Universal Gravitation, and the Second Law of Motion. The Universal law of motion says that force (F) of attraction between two objects of known mass is directly related to the product of the two masses (Mm) and inversely related to the square of the distance separating their midpoints, Equation 1 (Blakely 1996). Therefore, the larger the separation of the two centres of mass, the smaller the pull between them.

$F = G\frac{Mm}{R^2}$…..…… (1)

Where,

F - Force of attraction,

G - Represents a constant (6.67 x 10-11 Nm2kg-2),

Mm - Denotes the two masses, M is mass of the earth while m is mass of the anomaly,

R^2- Distance between the two masses.

Newton's 2nd law of motion states objects of acceleration is a ratio of the net force acting on it and the objects mass, a=F/m. However, this is usually redone to a more universally accepted and familiar form as shown in Equation 2. When the acceleration (a) is due to gravity, then the force in a vertical direction and hence a in a=F/m is replaced with g to imply acceleration due to gravity. Theoretically, this law can therefore be given as follows:

F = mg …..…… (2)

Where,

F - The attraction force,

m - The objects mass,

g – Acceleration as a result of gravity.

When equations 1 and 2 are combined (Equation 3), another simple relationship is obtained (Equation 4):

F = $G\frac{Mm}{R^2}$ = mg ...…… (3)

thus;

$$g = \frac{GM}{R^2} \quad \text{..... (4)}$$

This clearly demonstrates that the scale of acceleration owing to gravity on Earth, g, is a ratio of Earth's mass (M) and the square of its radius (R). Hypothetically, acceleration owing to gravity would be constant over the Earth but ideally is not. In real world however, gravity differs from place to place since the earth is spherical, it rotates, and has an uneven outward topography and inconsistent mass distribution. The default value of g on Earth's surface is 9.8 m/s^2. The c.g.s. unit of acceleration due to gravity is Gal; this was adopted in honour of Galileo Current gravimeters can measure exceptionally minor differences in acceleration due to gravity. The sensitivity of these instruments is roughly ten ppm (Blakely 1996).

2.5.2 Applications

In geothermal surveys, the principal aim of acquiring and analysing gravity data is to bring improved knowledge of the subsurface geology (Hinze 1990). This technique is comparatively inexpensive and environmentally friendly remote sensing method. This method does not require putting of energy into the ground for purposes of obtaining data; consequently, the technique is very appropriate for a populated locale.

Differences in the Earth's gravitational field are triggered by variations of sub-surface rock density. Gravity technique has been used widely in search for oil and gas mostly in the twentieth century. In a report published by Reynolds in 1977, gravity method has other applications namely: regional geological studies, isostatic compensation determination, hydrocarbon surveys and mass estimation of mineral deposits, detection of subsurface cracks, location of concealed rock valleys, determination of glacier thickness, tidal oscillations, archaeo-geophysics, geodesy, changes in water table levels, identification of

buried groves, caves, sinkholes and near-surface faults, military especially in missile trajectories and deformation monitoring.

Gravity method works when objects below the earth's surface bear different masses, which reflects objects having different density from the surrounding material. However, the measured earth's gravitational field is affected in various ways by the earth's shape and rotation, earth tides and topographic changes which have to be eliminated before interpretation. This method has better depth of penetration as compared to, EM methods and ground penetrating radar.

2.6 Previous works

The rift valley is characteristic of surface indicators such as altered grounds, fumaroles and hotsprings. Previous researchers have described the origin of these features in similar ways. The findings by previous researchers are discussed as per the respective method, namely: gravity, seismology and EM. According to (Searle, 1970), the anomaly is a high dense intrusion originating from the mantle and has a width of 20 km spreading from 20 km deep. Hearly, 1975 explained that a system as such would have its source of heat associated to arising dyke from an intra-crustal magma reservoir. The rift axis was said to be associated with an intermittent narrow positive anomaly running from Lake Turkana to Lake Magadi in the south with varying width and amplitude.

The long-lived trachytic volcanism in the rift was explained by subsequent fractional crystallization of basalts, without the necessity of transverse structures facilitating magma ascent (Leat, 1991). The presence of hot mantle material beneath the Kenya dome since the onset of volcanism here at 15-20 ma was discovered to still be well-matched with the sudden change in mantle longitudinal wave velocities as the rift margins are intersected (Mechie et al., 1997).

Gravity maps of the central Kenya Rift show a long-wavelength bouguer anomaly minimum and axially aligned short-wavelength highs (Swain et al. 1994; Simiyu and Keller 1997; 2001). All late Quaternary trachytic volcanoes, including Menengai and Ol'rongai, are distributed along positive anomalies, rather than along the young, regional-scale left-stepping faults. Detailed analysis of gravity data showed anomaly with an amplitude of 30 milliGal, half-wavelength of 15 km and a NW-SE trending anomaly interpreted to be related to the heat source (Simiyu and Keller, 1998). Band pass filtering indicated that the NE- SW trending anomaly has two maxima with amplitude up to 15 and 24 mGal. They also identified linear positive anomalies showing control of structures in the basement and shallow bodies related to Menengai volcanic activity. During this study, a basaltic melt magma body was postulated as the main heat source directly beneath the caldera. Gravity data interpretation by analysis Bouguer anomaly map indicated presence of a high density body in the central part of the caldera (Figure 4). Since the volcano is relatively young this body could still be hot, the heat being conducted to near surface regions by dykes (Mariita et al., 2004). Tectonic activities affect geological landscape physically in the subsurface. These activities causes among others tension, compression and bending leading to fracturing of rocks (Hasanah et al., 2016).

Regional seismic studies of the crust along the Kenyan rift, showed significant differences in crust structure between the northern, Central and southern parts of the rift valley (Simiyu and Keller, 2001). The rift fill thickness varies from 1.5 km to 5 km underlain by basement material of velocity 6.05 km/s. High velocity bodies associated with the Menengai, Olkaria and Suswa Quaternary volcanic centres were mapped (Figure 5).

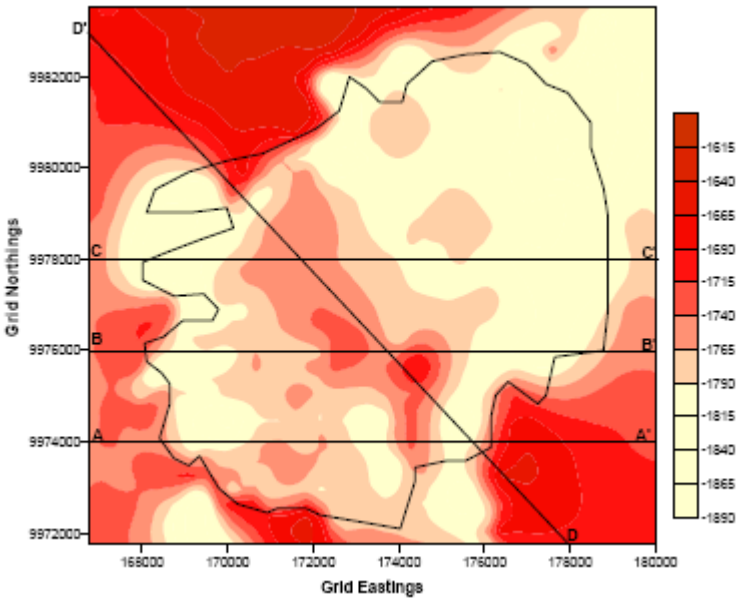

Figure 4: Bouguer anomaly map of Menengai area. The line running from east to west and the one running from the North West to South East are profiles (Mariita et al., 2004).

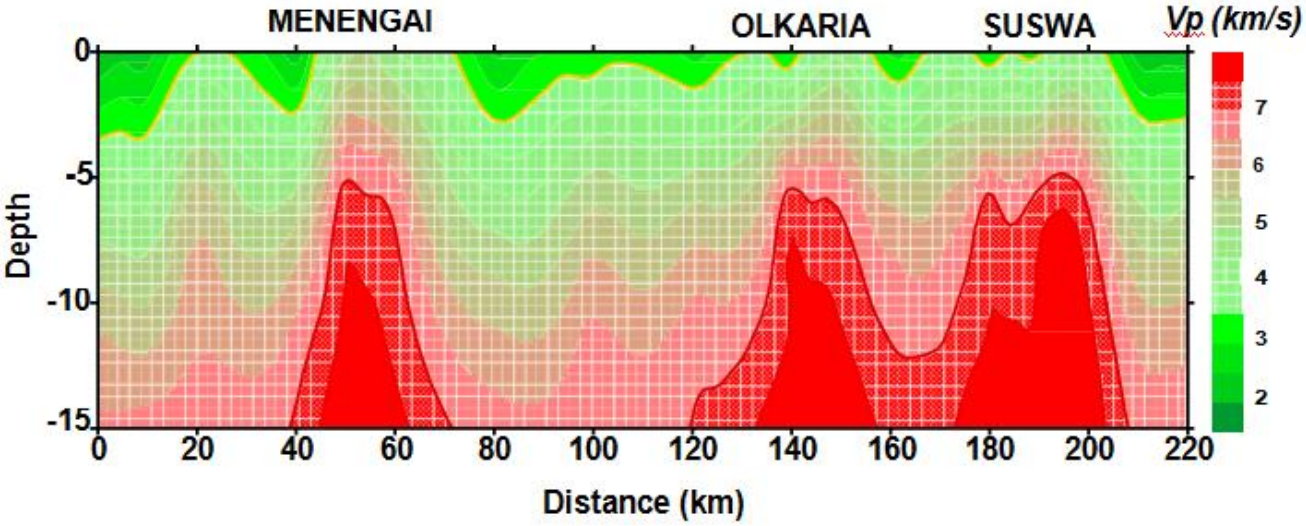

Figure 5: Seismic Velocity model along the Rift axis showing high velocity zones beneath Menengai, Olkaria and Suswa Volcanic centers based on the KRISP 1985-1990 axial model by Simiyu and Keller, 2001.

Magnitude-distance distribution for earthquakes have a greater proportion of the smallest earthquakes of magnitude 1.5 and less are recorded very close and within the network centre but fewer and larger magnitude 1.5 and greater on the periphery. This result is similar to recording in other high temperature and pressure geothermal fields such as Olkaria, Kenya (Simiyu and Keller, 2001 and (Stroujkova & Malin, 2000). The amplitude and depth of the seismic activity peak is predicted to decrease with increasing geothermal gradient.

Earthquakes represent a sudden slippage of rock along a fracture surface and generally should be restricted to a zone of brittle deformation. The maximum depth in a region at which earthquake intensity peaks will delineate the brittle-ductile transition zone, (Meissner & Strehlau, 1982). It was suggested that stress along the rift floor in the Central Kenya Rift area was being released by micro-seismic activities in geothermal areas but by larger earthquake sequences along the rift boundary faults (Fairhead and Stuarts, 1982). This interpretation was also supported by recent seismic intensity, magnitude and depth distribution analysis in Lake Bogoria and Olkaria (Young et al, 1994 and (Simiyu, 1999). It was alluded that geothermal fields owe their existence to the presence of molten rock in the crust.

The location of these bodies in many fields has been mapped by analyzing regions of high S wave attenuation. It was realized there were diminished S wave amplitudes in some of the seismograms and spectral analysis of arrival times and first motion showed that the signals were of low dominant frequencies less than 3 Hz (Simiyu & Keller, 1998) . This was taken to imply that the rays were passing through a molten body or less compacted low velocity material near surface. This either suggests the axial intrusion of magma or the significance of intra-rift horst blocks to influence the gravity signal, (Simiyu and Keller 2001). Another suggestion was made by that there exist intrusions below the Menengai,

Olkaria and Suswa volcanoes as shown in the Bouguer map (Figure 6).

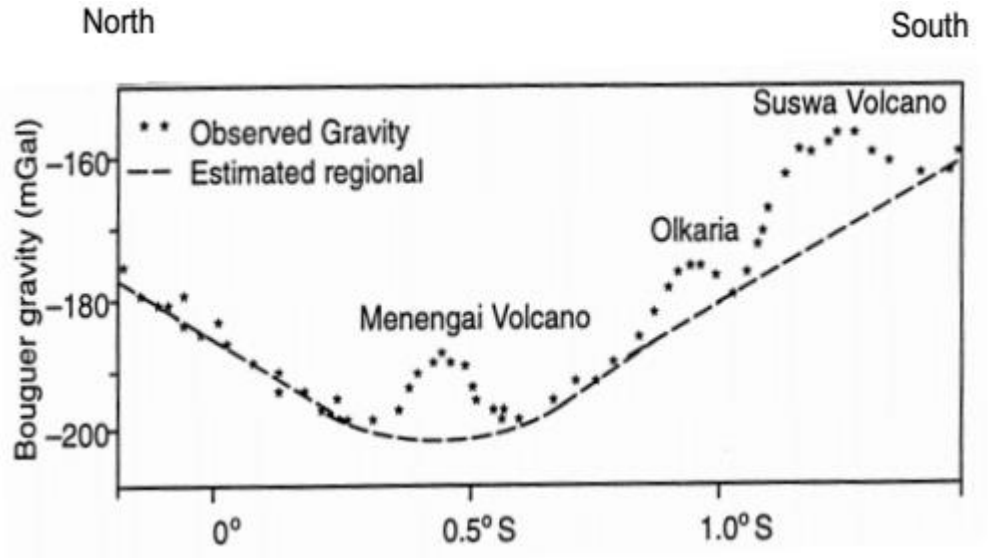

Figure 6: Anomalous bodies below Menengai volcano (Simiyu and Keller 2001).

Bouguer results showed a positive gravity anomaly in the middle of the caldera (Figure 7), which was interpreted as a magmatic intrusion (Wamalwa 2011; 2013).

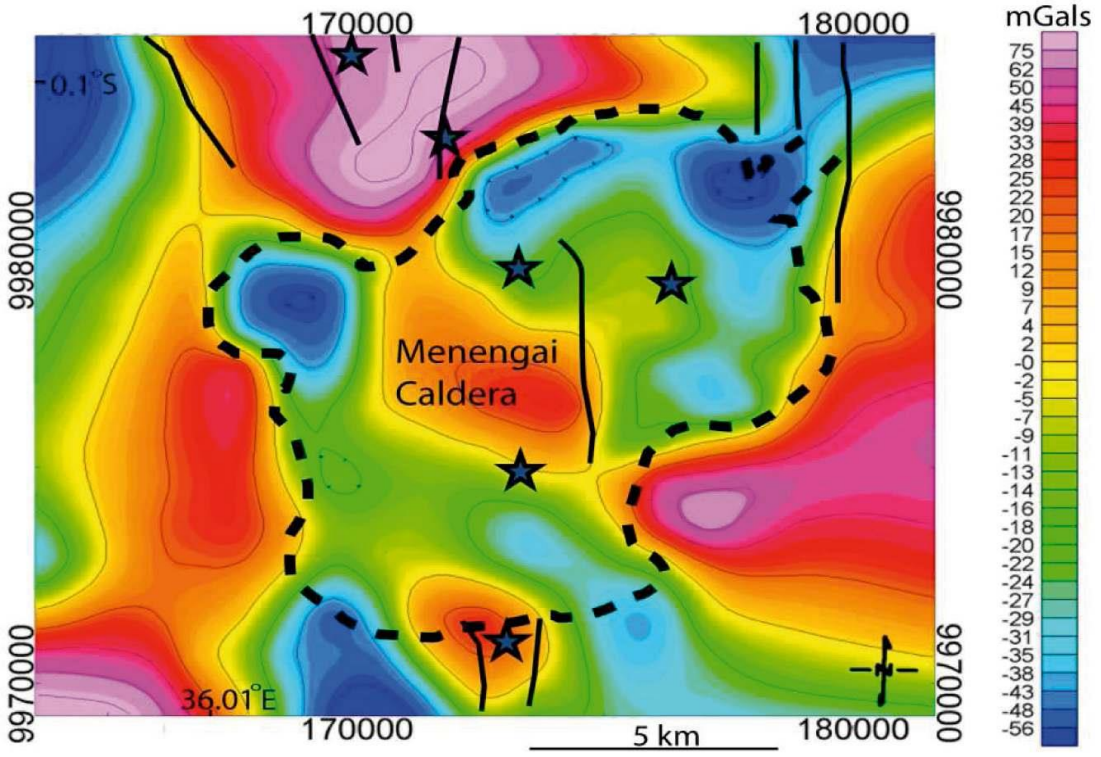

Figure 7: Bouguer anomaly of Menengai (Wamalwa 2011; 2013).

These studies led to a conclusion that the central-caldera structures were incompatible with the remainder of the structural inventory and thus were interpreted to reflect a local, magmatically driven stress-field perturbation.

Measurements and modelling of magneto telluric data recorded a less resistive zone at a depth of 3 km (Figure 8), this was associated with a molten body (Wamalwa 2011; 2013). It therefore appears likely that the observed structures are the direct result of magmatic addition into the shallow parts of the crust, associated with localized growth of topography and the generation of local structures, independent of the regional tectonic stress field.

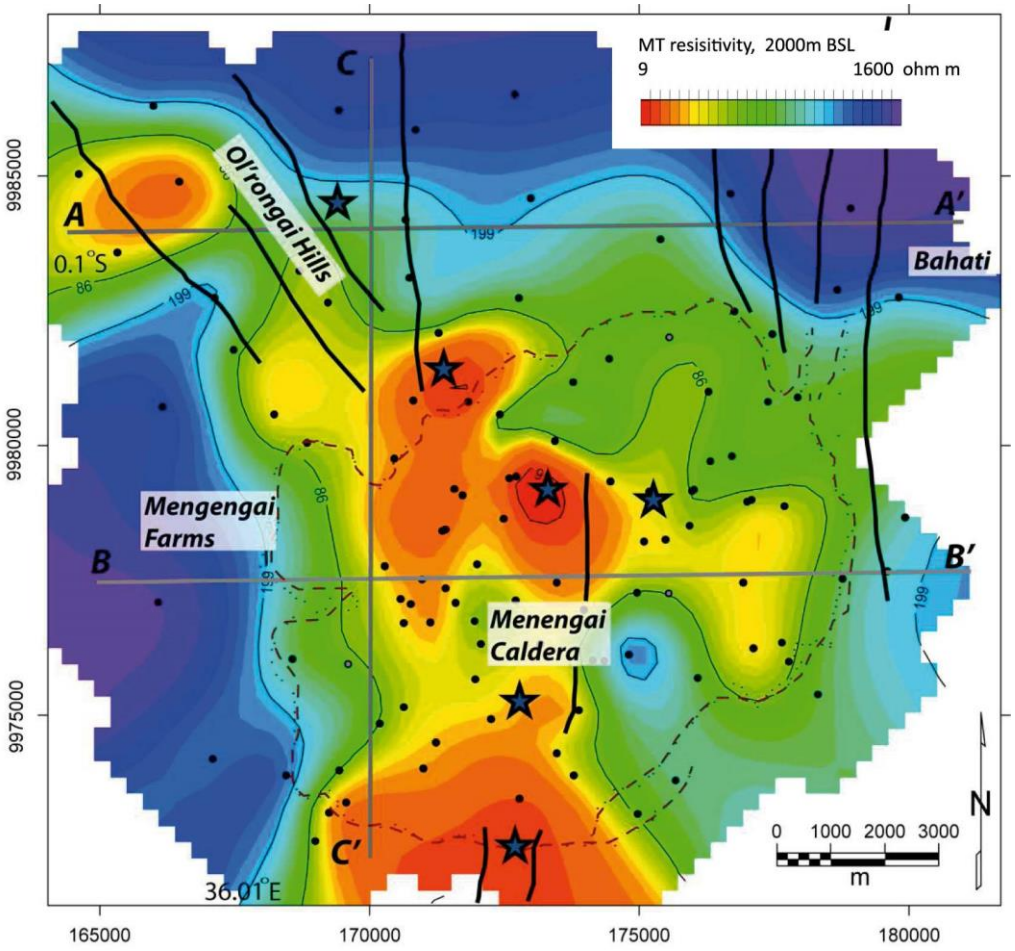

Figure 8: Resistivity map of Menengai at a depth of 3 km below surface (Wamalwa 2011; 2013).

The interest to do more research and reinterpretation of gravity data was reignited by the renewed interest by the government of Kenya to explore geothermal resources in Menengai caldera and by the fact that all the previous researchers focused mainly on the intrusion and therefore the author of this research work found a gap where permeability was not taken as serious a component as in geothermal exploration.

CHAPTER THREE

3. RESEARCH METHODOLOGY

3.1 Introduction

This chapter covers the research design adopted for the study which is a case study of a geothermal field in Kenya. The raw gravity data used for this study was obtained from Kengen and GDC. This raw data was then subjected to reduction procedures to simple Bouguer and thereafter several filters were applied to achieve the set objectives. The reduction procedures are discussed in this chapter, section 3.5.

3.2 Research Design

The design of experiment for this research was a quantitative descriptive case study of Menengai geothermal field aimed at developing structural models, establishing whether there is permeability and to test the relationship between gravity derived structural models to those of EM method. The data used was collected in the period between years 2001 and 2015 by Kengen and GDC.

Table 1 is a sample of the data used while the rest of the data is contained in the appendix.

Table 1: Sample data showing in summary the data that was the backbone of this survey.

Eastings	Northings	Elevation	SBA		Eastings	Northings	Elevation	SBA
156700	9982130	1843	-1819		170590	9998680	1614	-1658
156700	9983380	1824	-1813		170610	9999300	1594	-1659
156750	9998600	1655	-1680		170620	9999150	1596	-1664
156930	9979050	1914	-1837		170630	9997100	1680	-1660
156930	9988930	1719	-1714		170650	9974350	2010	-1794
156950	9987500	1737	-1752		170680	9985950	1746	-1598
156960	9977710	1937	-1861		170680	9997590	1673	-1654

157050	9973530	2035	-1888		170685	9975467	2032	-1773
157050	9984610	1800	-1797		170710	9997710	1665	-1655
157050	9991730	1679	-1733		170720	9985360	1775	-1583
157130	9980280	1880	-1846		170720	9997980	1639	-1660
157150	9983250	1821	-1814		170730	9986270	1743	-1602
157180	9981990	1846	-1816		170730	9992630	1648	-1663
157200	9982500	1836	-1812		170750	9980300	2019	-1706
157200	9990000	1700	-1702		170750	9997960	1640	-1660
165200	9969900	1919	-1660		175810	9989110	1745	-1748
-	-	-	-		-	-	-	-
-	-	-	-		-	-	-	-
-	-	-	-		-	-	-	-
165200	9984300	1791	-1678		175860	9987970	1767	-1742
165200	9991180	1654	-1602		175860	9988650	1759	-1746
165200	9991180	1654	-1602		175870	9987490	1770	-1734
165220	9989790	1697	-1582		175880	9989590	1738	-1756
165230	9983100	1823	-1723		175880	9975053	1974	-1807
165230	9983100	1823	-1723		175886	9977809	1925	-1811
165250	9974110	2029	-1767		175900	9998680	1718	-1754
165260	9977700	1992	-1766		175902	9971337	2105	-1806
165280	9988510	1721	-1583		175920	9983730	1865	-1711
165280	9993800	1615	-1613		175931	9981556	1826	-1805
165300	9975300	2025	-1770		175946	9972677	2250	-1805
165390	9980630	1941	-1745		175950	9992200	1684	-1772
165410	9988410	1724	-1581		175984	9975350	1981	-1808
165480	9984700	1791	-1653		176010	9990140	1722	-1770

3.3 Reliability and Validity

Reliability is concerned with questions of stability and consistency. It is the degree to which a study tool steadily yields results persistently. In the field, data is acquired in stacks of three per station which helps in reliability and reproducibility check. Once the data is downloaded to a computer, it is opened in Microsoft Excel for manipulation and sorting. The stacks are then compared and the one with the lowest standard deviation is preferred to the other two. Next the gravimeter tilt check is done for the three stacks downloaded and the stack with the smallest XY tilt value is preferred to the other two.

The gravity meters used in data collection have a spring constant which is regularly determined by simply repeating measurements at the same stations at different times of the day. This corrects for instrument drift and earth tides.

Validity test of a data collection instrument enables us to ascertain that we are measuring the correct concept. To validate the data, surface structural features and gravity structural models were overlain and the rim of the caldera featured conspicuously in all. This check confirmed that the measuring instrument was able to access the right concept. This was demonstrated in Chapter four in all figures.

3.4 Instrumentation

The instrument for measuring the variation of the earth is called a gravimeter. There exists two types of gravimeters, absolute and relative meters. The latter measures relative changes in g between two points while the former measures actual value of gravitational acceleration by measuring the speed of a falling mass using a laser beam.

Figure 9: A photo of Scintrex CG-5 relative gravimeter

For the relative meters, two equipments are recommended where one remains stationed at the base station so as to continuously adjust for the drift correction while the second meter is used as a rover. The rover is used to collect data from one station to another. In case only one meter is available, the same equipment is used as a rover for collecting data from station to station while still visiting and taking a reading at the base station after every 1-2 hours. A base station is a point whose absolute value is known and it is from this that the absolute values for all other stations are calculated.

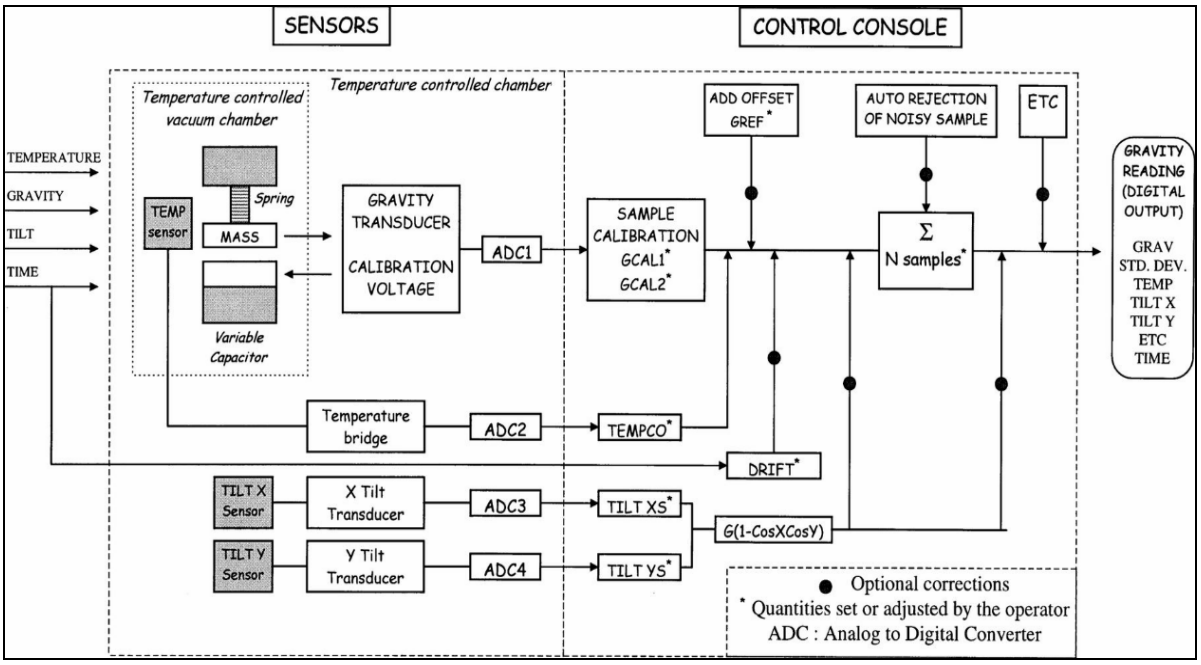

Figure 10: Acquisition scheme for the Scintrex (Bonvalot et al., 1998, modified from Scintrex 1995).

The acquisition scheme is divided into sensors and control console (Figure 10). The sensors part consists mainly of elements that detect density variations, temperatures changes, equipment tilts and time. These elements detect physical signals which are then converted to active circuit signals by the transducers. These signals are in analog mode and are therefore converted to digital format by the analog to digital converters (ADCs).

TEMPCO is the temperature correction factor determined by the manufacturer. GCAL 1 and GCAL 2 are the first and second-order calibration factors of the gravity signal and DRIFT is the correction factor used for the instrumental linear drift correction.

The control console consists of elements that require adjustment by the operator. The parameters TILT XS and TILT YS are the tilt sensor sensitivities adjusted by the operator while ETC is the software-computed Earth tide correction based on the Longman algorithm. The final output is the Gravity reading and parameters that affects that reading which includes: Standard Deviation, Temperature, ETC, Time and Tilts (X and Y).

3.5 Data Acquisition

The following are steps involved in design and gravity data collection from identification of the study area to actual data collection in the field:

The first step involves identification of the survey area. For this case, the area identified for this study is Menengai. The second step in data collection involves Drift calibration of the gravimeter. Drift calibration is done to ensure that the equipment stabilizes to the original settings of the creeping spring. Once drift calibration is done, the next step involves identification of an absolute gravity station whose absolute gravity value is known. This is important in order to calculate the absolute gravity values for the survey stations. Next is setting up of a base station which is done to perform drift correction of the data on a day to day basis without which gravity data would be impractical and hence unreliable. The base station should be in an accessible place and should be a little bit outside the survey area in a geologically stable ground and quiet area away from the noise of GPS and gravity stations. Once the base station is setup, field data collection can now begin.

These processes are illustrated as shown in the following flow diagram (Figure 11).

When the actual data acquisition begins, the first thing to is to take a gravity reading at the base station in the morning and then proceed to individual gravity stations and finish in the evening at the same base station. At each gravity station, the height of the gravimeter, the gravity reading, standard deviation, tide, time, date and station name were recorded in a field note book in addition to the saving data in the gravimeter for retrieval later. Information on the latitude, longitude and elevation for each reading station was also recorded using a differential GPS for greater accuracy.

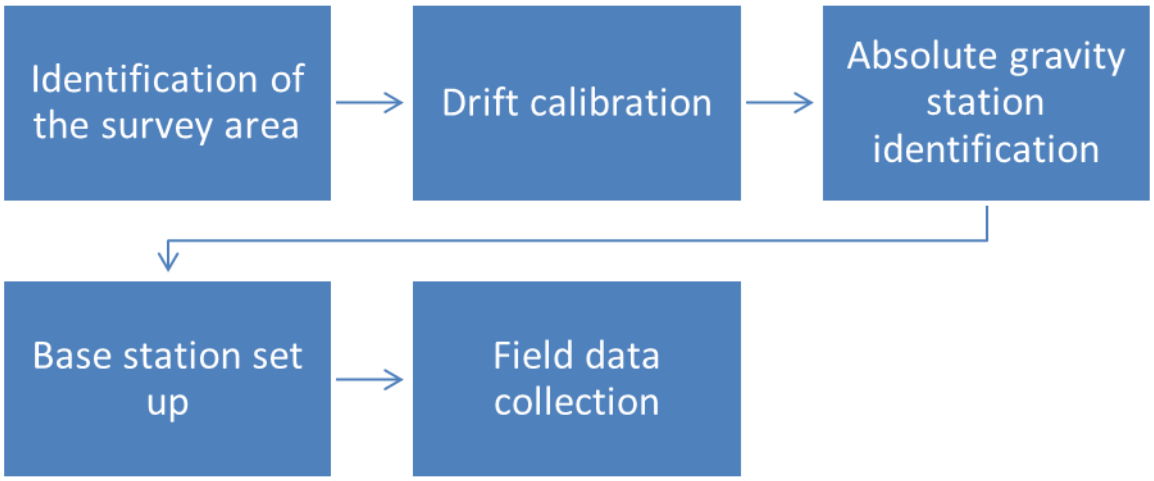

Figure 11: A flow diagram illustrating gravity data acquisition processes.

Desktop studies were carried out and it was established that Kengen and GDC had already done extensive gravity data acquisition in the area. The source of raw gravity data for this study was therefore acquired from these two state corporations.

Figure 12 is an illustrative drawing showing measurements and indicates the comparative surface difference of gravitational acceleration related to subsurface features. When the craft flies above a heavier rock mass, the gravitational pull increases above normal while the curve above reflects the gravity behaviour.

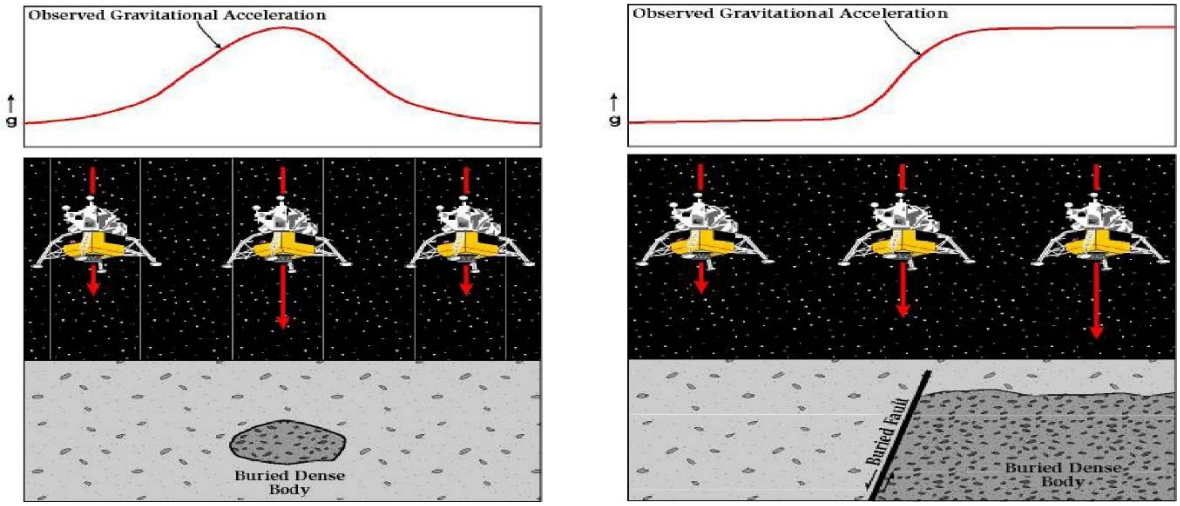

Figure 12: Graphics illustrating relative surface difference of gravitational acceleration over masses of varying densities.

3.6 Reduction Procedures

When a reading is recorded, it is multiplied by an instrumental calibration factor to produce a value of observed gravity (gobs) since meters do not record direct gravity measurements. The correction process is known as gravity data reduction or reduction to the geoid. The various corrections that can be applied are the following:

Instrument drift - Gravimeter readings change (drift) with time as a result of elastic creep in the springs, producing an apparent change in gravity at a given stations. The

instrumental drift can be determined simply by repeating measurements at the same stations at different times of the day, typically every 1 – 2 hours.

Earth's tides - Just as the water in the oceans responds to gravitational pull of the Moon, and to a lesser extent of the Sun, so too does the solid earth. Earth tides give rise to a change in gravity of up to three gravity units with a minimum period of about 12 hours. Repeated measurements at the same stations permit estimation of the necessary correction for tidal effects over short intervals, in addition to determination of the instrumental drift for a gravimeter.

Observed gravity (Gobs) - Gravity readings observed at each gravity station after corrections have been applied for instrument drift and earth tides.

Latitude correction (Gn) - Correction subtracted from gobs that accounts for Earth's elliptical shape and rotation. The gravity value that would be observed if Earth were a perfect (no geologic or topographic complexities), rotating ellipsoid is referred to as the normal gravity.

Gn = 978031.85 (1.0 + 0.005278895 sin2 (lat) + 0.000023462 sin4 (lat)) (mGal)..... (5)

Where,

Lat - is latitude Free-air corrected gravity (gfa) - The free-air correction accounts for gravity variations caused by elevation differences in the observation locations.

Free-air gravity anomaly - The free-air correction accounts for gravity variations caused by elevation differences in the observation locations (gfa) is given by:

Gfa = gobs – gn + 0.3086h (mGal)..... (6)

Where, h is the elevation (in m) at which the gravity station is above the datum (typically sea level).

Bouguer slab corrected gravity (gb) - The Bouguer correction is a first-order correction to account for the excess mass underlying observation points located at elevations higher than the elevation datum (sea level or the geoid). Conversely, it accounts for a mass deficiency at observation points located below the elevation datum. The form of the Bouguer slab corrected gravity, *gb* is given by:

Gb = gobs - gn + 0.3086h - 0.04193r h (mGals)..... (7)

Where r is the average density of the rocks underlying the survey area.

Terrain corrected bouguer gravity (gt) - The terrain correction accounts for variations in the observed gravitational acceleration caused by variations in topography near each observation point. Because of the assumptions made during the Bouguer Slab correction, the terrain correction is positive regardless of whether the local topography consists of a mountain or a valley. The form of the Terrain corrected, Bouguer gravity anomaly, gt, is given by:

Gt = gobs - Gn + 0.3086h - 0.04193r h + TC (mGal)..... (8)

Where TC is the value of the computed terrain correction.

After accounting for all these variations accurately, the rest is expected to be caused by subsurface structures Equations 5-8 have been modified from (LaFehr 1991).

Bouguer anomaly - The end product of gravity data reduction is the Bouguer anomaly which should correlate only with lateral variations in density of the upper crust and which is of most interest to applied geophysicist and geologists. The bouguer anomaly is the difference between the observed gravity value (gobs), adjusted by the algebraic sum of all the necessary corrections. The variation of the bouguer anomaly should reflect the lateral variation in density such that a high density feature in a lower-density medium should give rise to a positive bouguer anomaly (LaFehr 1991). Conversely, a low density feature in a higher density medium should result in a negative bouguer anomaly.

Once Bouguer anomaly has been achieved, trend surface analysis is done on the data and several filters applied to achieve the set objectives. The objective of trend surface analysis is to extract the long wave component of the Bouguer anomaly derived from the deep subsurface composition. Trend surface is obtained by approximating the long wave component of the Bouguer anomaly by the n-order curved surface. Trend analysis is a directional filter to enhance particular strike direction (Figure 13).

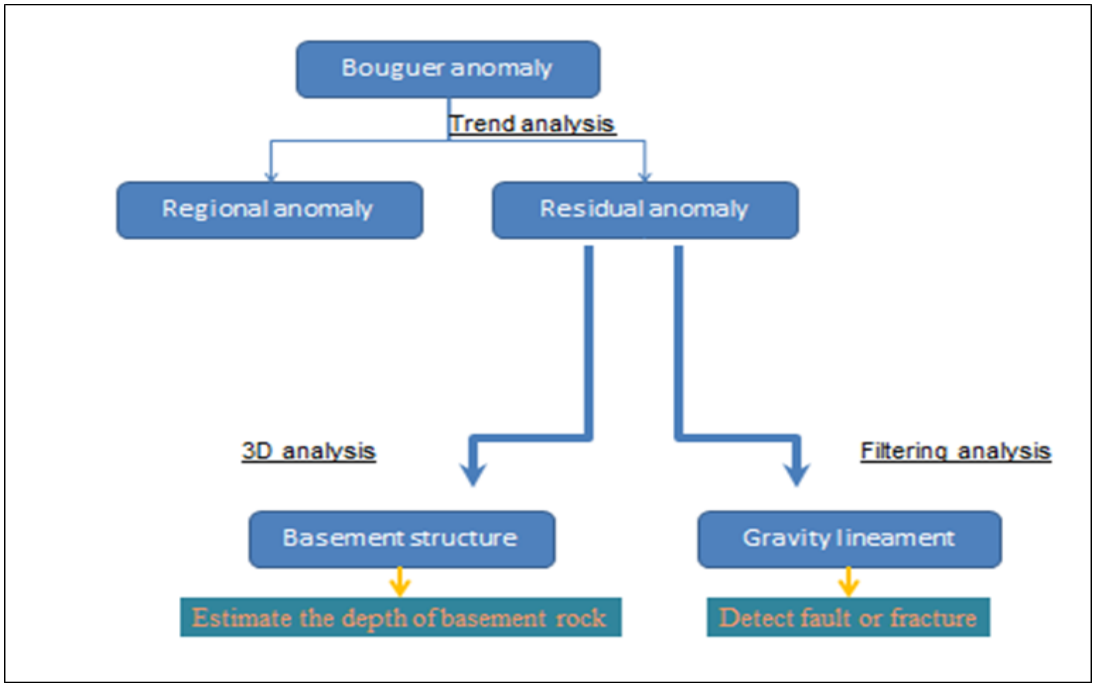

Figure 13: General flow of Gravity analysis.

After separation of long wavelength from the short wavelength, the resultant data is specific to the particular area of interest without influence from the regional dynamics. The data was loaded to surfer platform, a program by golden software for gridding to develop Gravity structural models. The gridding method applied for data that is well distributed in an area is called Kriging. This method is an advanced geostatistical procedure that generates an estimated surface from a scattered set of points.

On this platform, the data was further subjected to two filters namely: Band pass filter; applied to remove certain wavelengths, horizontal derivative filter; applied to image zones of sharp contrasts. These two filters helped in identification of structures responsible for permeability in Menengai geothermal field.

CHAPTER FOUR

4. RESULTS AND DISCUSSIONS

4.1 Introduction

The main focus of this study was on the production depth where permeability is expected to be more pronounced. This chapter therefore discusses results with respect to permeability controls in the area of study. Bouguer anomaly map was developed with all the necessary reductions applied and subsequent filters applied to achieve the set objectives.

4.2 Discussions

The Bouguer anomaly map that was developed shows an almost complete circular gravity low within the caldera associated with permeability and notable relative high gravity in the central part of the caldera (Figure 14). The high amplitude gravity gradients in this map could indicate contact zones that separate this high gravity anomaly and the faulted zones. The dense body in the central part of the caldera coincide with the dome area. It is deduced that this anomaly represents a magmatic intrusion. To perform trend surface analysis, band pass filter was applied to filter low and high wavelengths and this slightly improved interpretation.

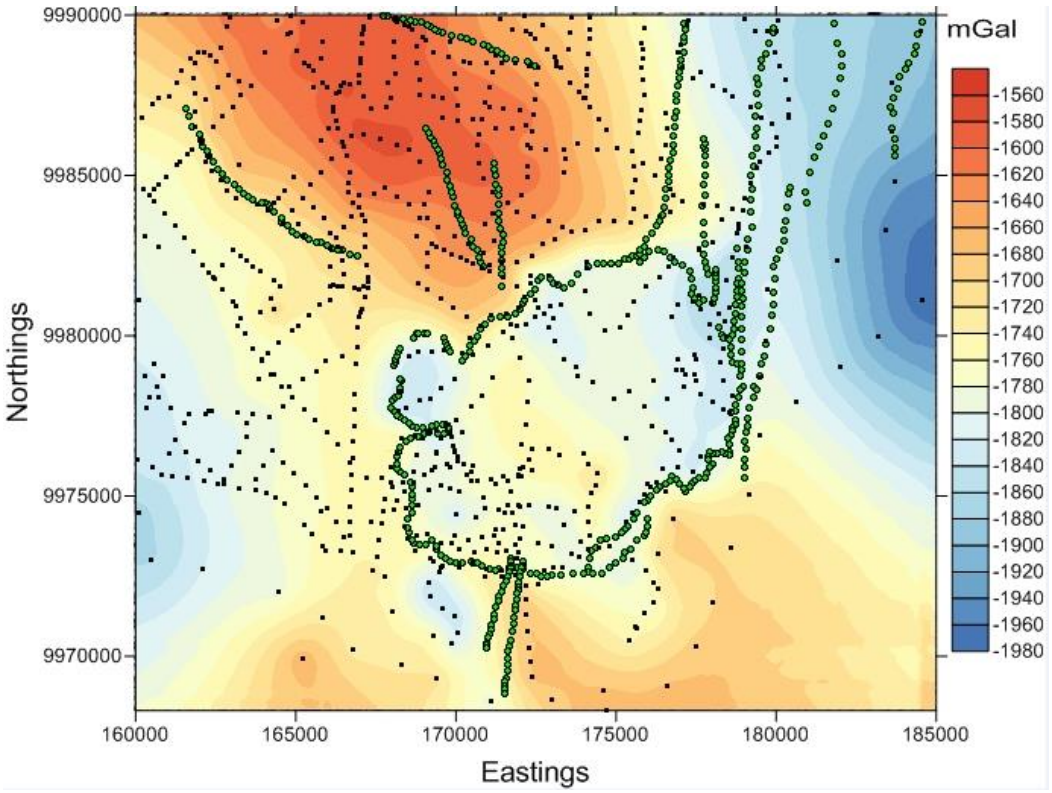

Figure 14: Gravity Bouguer anomaly map of Menengai Geothermal field. Black dots denote gravity sampling points.

A band pass filter of 50-3000 m was applied to the Bouguer data and some changes could be observed (Figure 15). This filter effectively removed the effect of deep seated dense bodies that had made the NNW part of the study area appear very dense in Figure 14. This study was interested with a depth of upto 3000 metres (m) and anything below this therefore had to be removed. The filter also removed any possible effect of surface bodies above 50 metres (m). Attempts to improve resolution further for better interpretation led to application of 100-3000m and 200- 3000 m filters (Figures 16 and 17) but this did not change the interpretation. To overcome this huddle, regional effects had to be removed and a residual gravity anomaly map was constructed. The regional effects had magnified short wavelength anomalies to deep seated anomalies leading to wrong interpretations and therefore had to be removed (Figure 18). The resulting residual anomaly map filtered these

effects leading to reduction in size of the highly positive anomalous body notable in the NNW orientation (Figure 19).

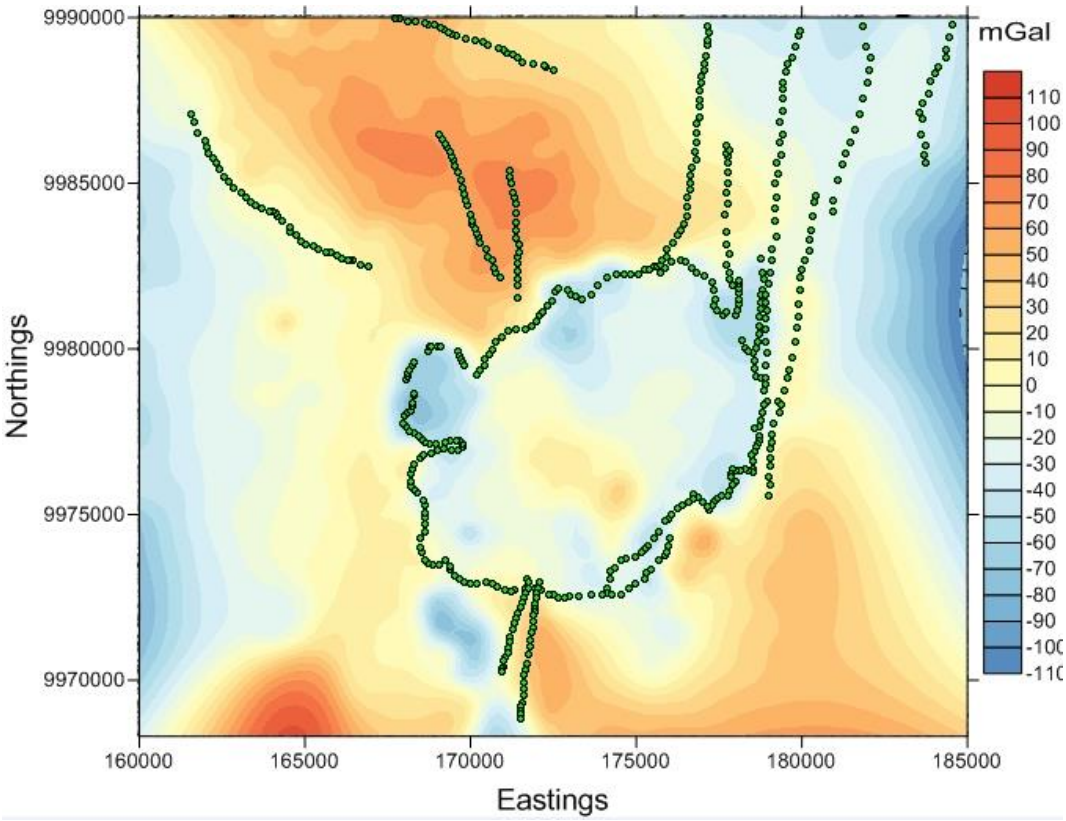

Figure 15: 50 – 3000 metres Band pass map of Menengai.

The importance of residual map is to remove the effects of Regional geology from the Bouguer map. The low gravity anomalies are associated to the axis of the caldera and Solai TVA to the NNE while the high anomalies are associated with dense magmatic bodies.

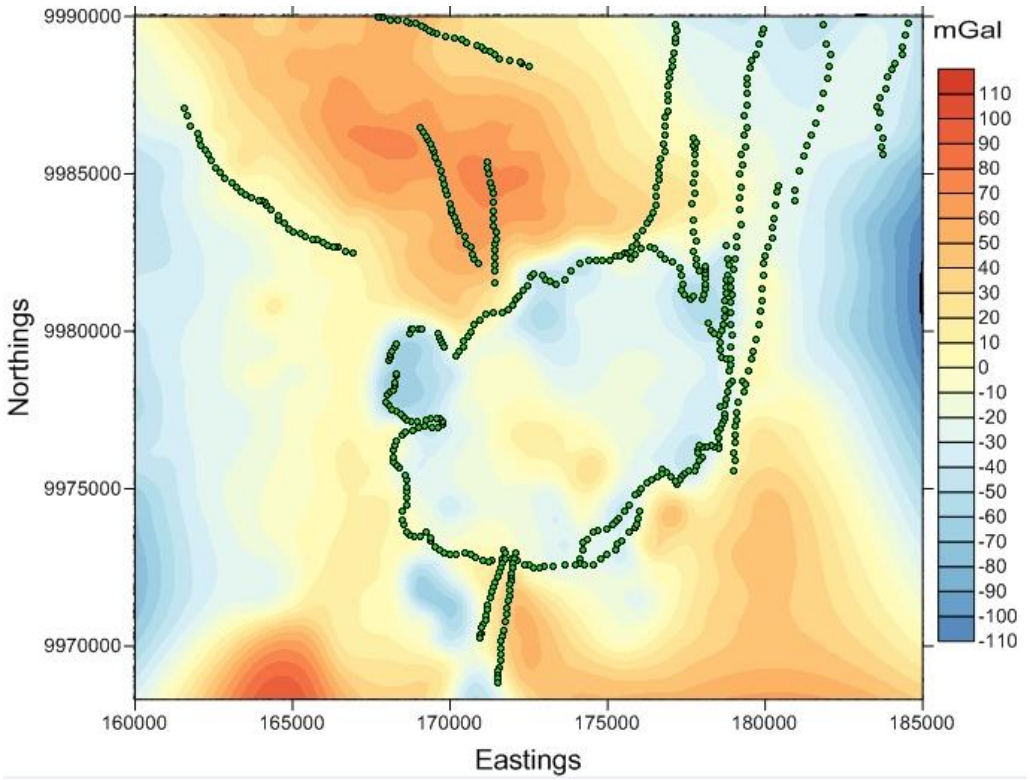

Figure 16: 100 – 3000 metres Band pass map of Menengai.

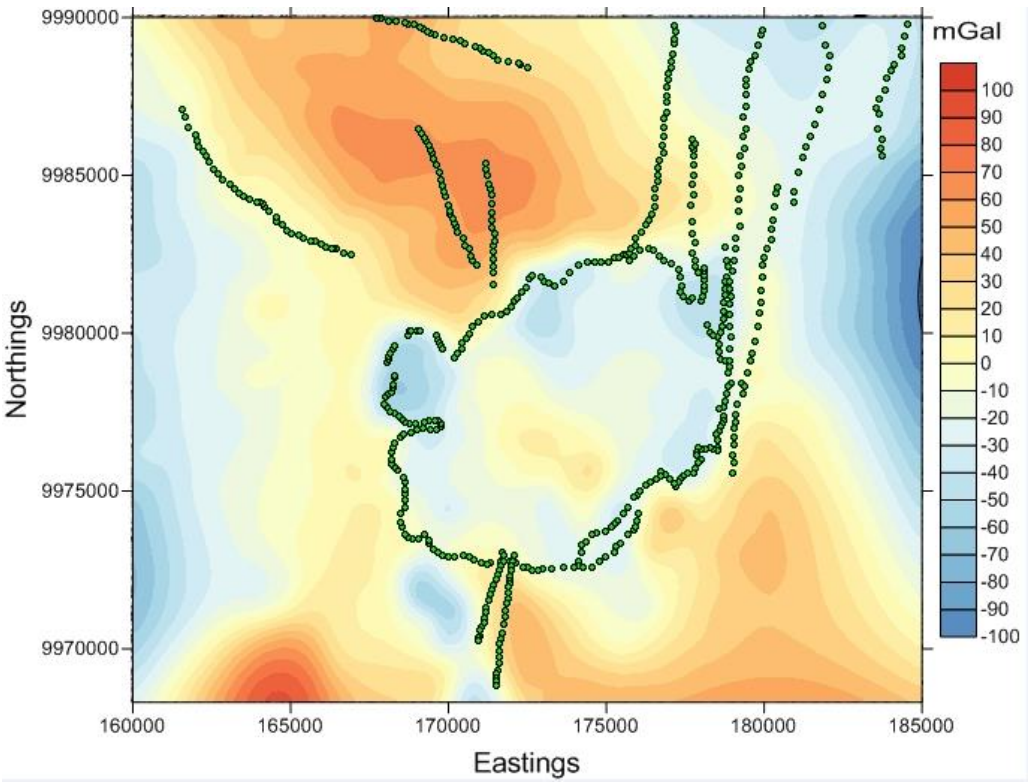

Figure 17: 200 – 3000 metres Band pass map of Menengai.

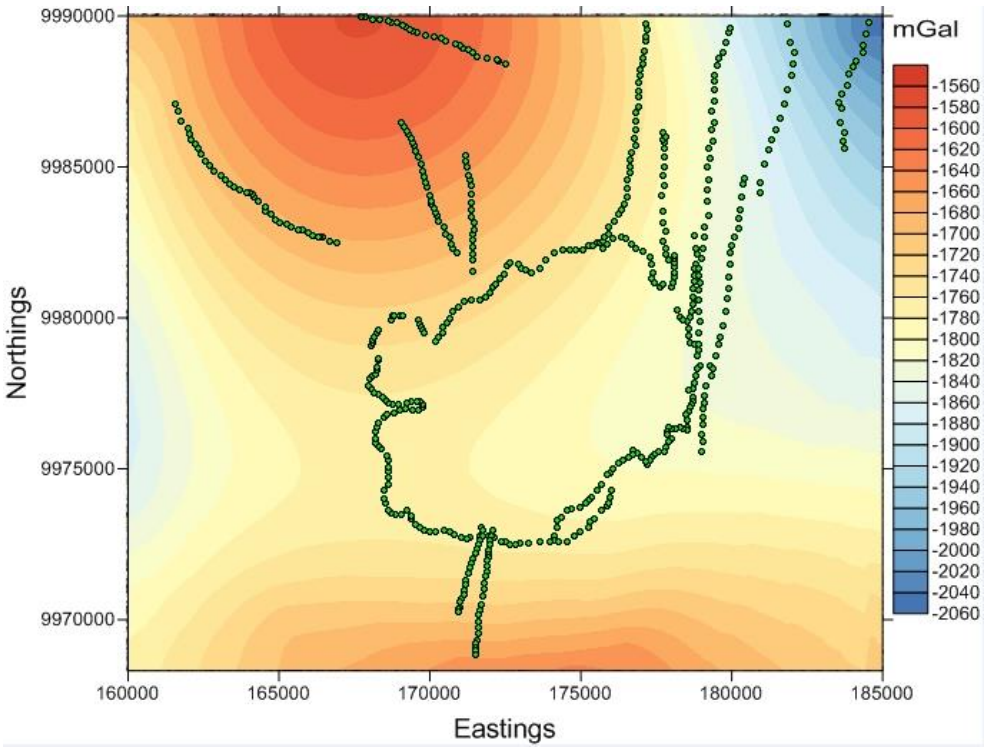

Figure 18: Regional anomaly map of Menengai Geothermal field.

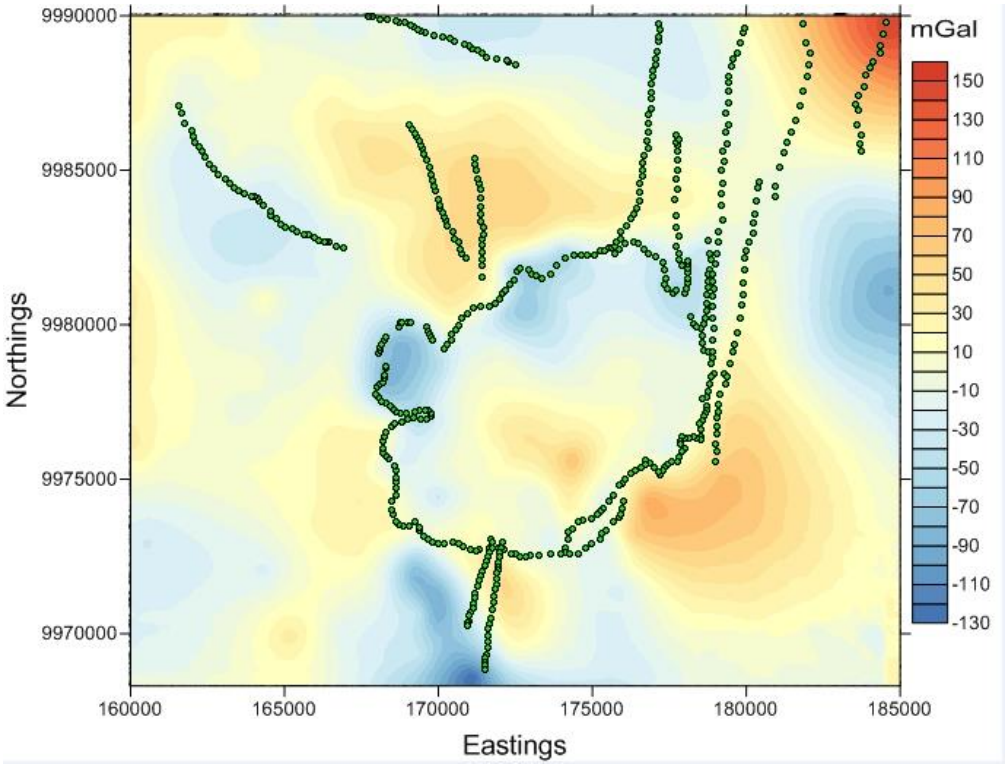

Figure 19: Residual anomaly map of Menengai Geothermal field

To improve clarity and establish whether there is enough permeability, more terrain surface analysis were carried out. 200- 3000 m Band pass filtered anomaly map was subjected to horizontal first derivative filter. This filter allows for better delineation of discontinuities by focussing mainly on the points of sharp gradients, thus delineating fractured zones (Figure 20). The same was done for the residual map and a map developed (Figure 21). These two figures show anomalous areas that are interpreted as local geologic features. The high amplitude gravity gradient which represents the major fault areas forms the basis of this research. These features are the highly fractured areas which are paths controlling fluid flow in and out of the caldera. The axis of the caldera is one clear area where geology is in complete agreement with these findings. The Molo TVA is another clear faulted area while the Solai TVA could not be captured by this filter.

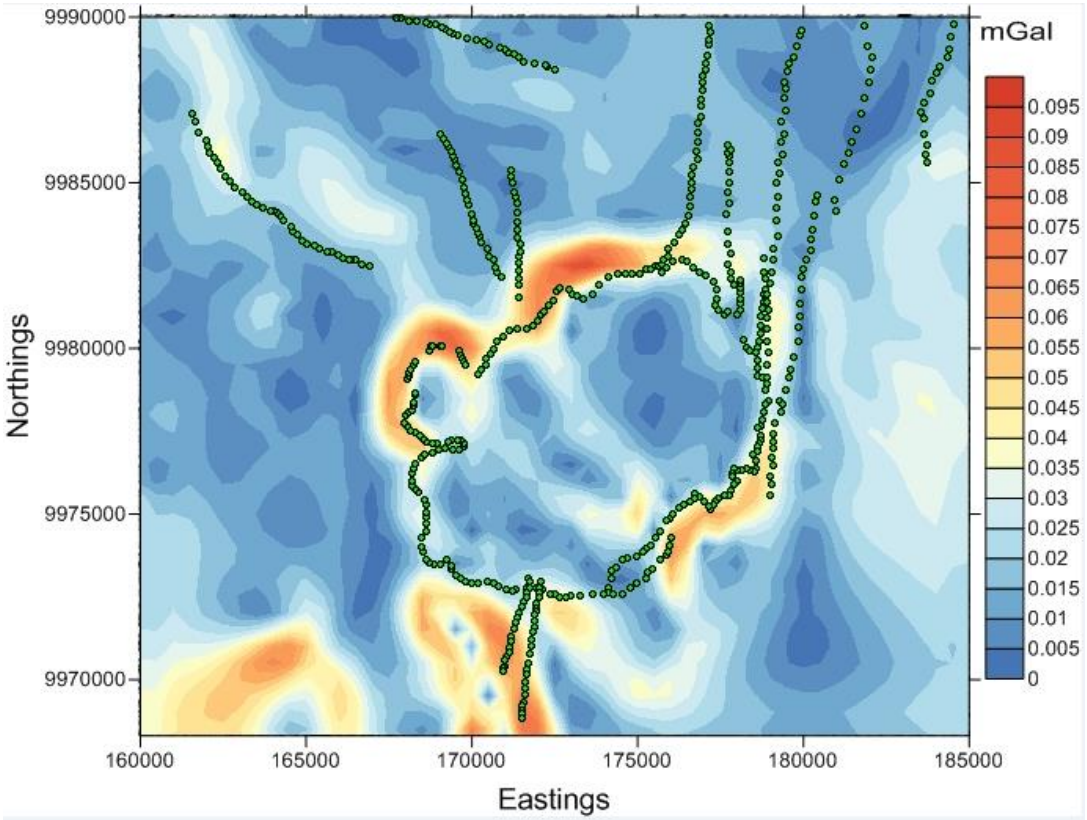

Figure 20: Horizontal derivative filtered 200-3000 Band Pass anomaly map of Menengai Geothermal field

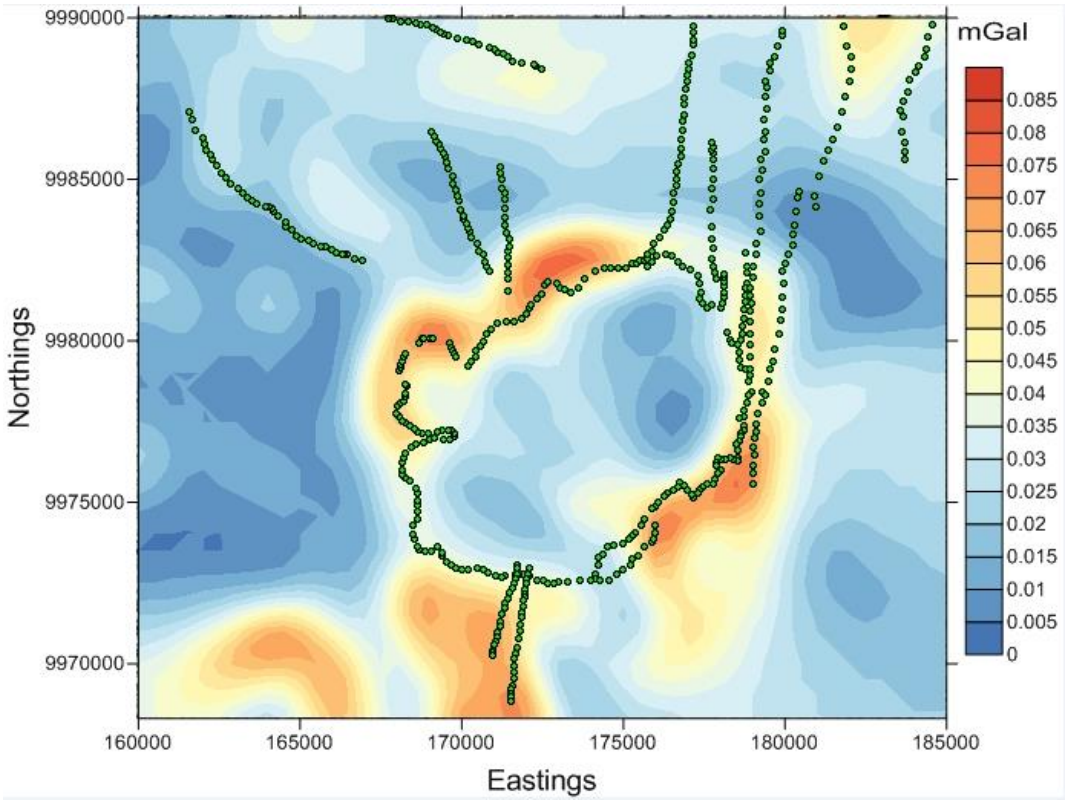

Figure 21: Horizontal derivative filtered Residual anomaly map of Menengai Geothermal field.

A comparison of gravity model (Horizontal derivative filtered 200-3000 BP anomaly map) with resistivity model (3 km) was done (Figure 22).

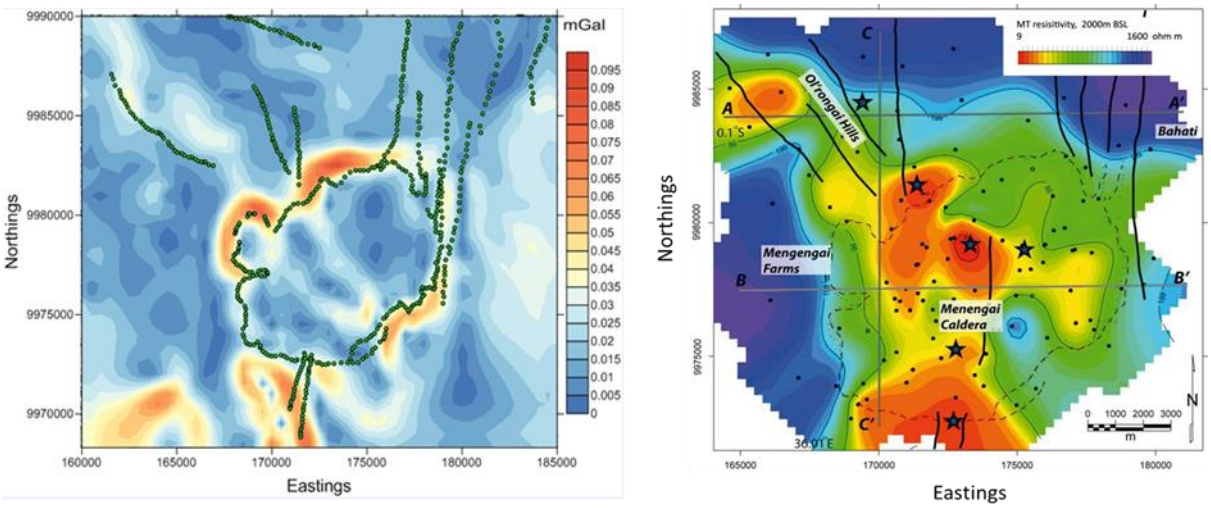

Figure 22: A comparison of Gravity model (left) with Resistivity model (right).

From the analysis of these two models, it was observed that gravity method is superior in identifying permeability controls as compared to the EM methods. Gravity model identified the rim of the caldera, Molo TVA and a fault structure to the south while resistivity model at the same depth, identified only the magmatic intrusion in the middle of the caldera. This shows how reliable gravity method would be in identifying surface and buried fractures as compared to EM methods if well used. On the same breath, gravity does not require a huge workforce to operate in the field as compared to resistivity.

Gravity measurements takes a short period i.e. three (3) minutes per sampling station while MT requires twenty one (21) hours so as to acquire low frequency data in the early morning hours. This shows that gravity method would acquire data over a large area within a shorter duration as compared to EM methods. A gravimeter can be handled by two (2) people in the field while MT would require at least four (4) people and seven (7) people for TEM respectively. This makes EM methods labour intensive, time insensitive and therefore gravity is the method for resource and better results sensitive exploration organisation.

Density inversion from results of simple Bouguer anomaly readings were generated by 3D inversion Grablox1.6 programme that calculates synthetic gravity anomaly of a 3D block model. The programme then generates files with inverted densities at each location where gravity readings were recorded with sets of varied depth. The inverted densities were then presented in 3-D visualization platform i.e. Voxler by Golden software (Figure 23). This figure summarises the results of gravity survey in mapping subsurface density contrast to locate structures (low density lineament) that channel geothermal fluids at depth in Menengai geothermal field. When density is set to zero (0) during filtering, it enhances the

contrast between negative and positive density boundaries at iso-dense contour of zero. The low density lineaments are fracture areas while the high density ones are intrusions. From this analysis, four groups of faults are identified, which include caldera rim faults that contribute mostly to deep vertical recharge, NNE-SSW faults along Solai graben, NNW-SSE faults along Molo axis and Southern fault extending towards Lake Nakuru.

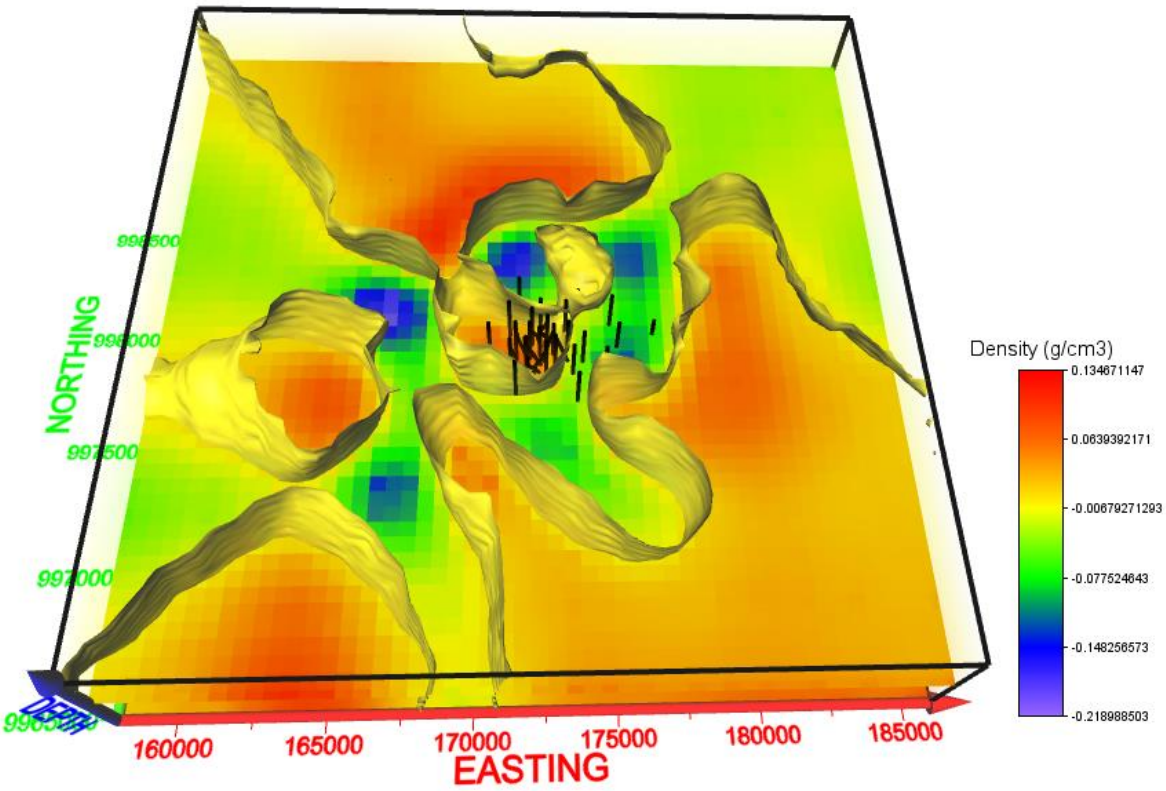

Figure 23: 3D iso-dense values at zero (0) to enhance structural boundaries.

CHAPTER FIVE

5. CONCLUSIONS AND RECOMENDATIONS

5.1 Introduction

The main objective of this study was to carry out gravity data modelling to understand density variations in the Menengai caldera and therefore uncover the subsurface structures with more focus on the fracture zones which acts as permeability controls. The particular goals of this study were:

i. To develop gravity structural models.
ii. To establish whether there is permeability in Menengai.
iii. To test gravity models with other existing resistivity models.

This chapter therefore explores the outcome of this research and whether the set objectives were achieved and then recommendations are given.

5.2 Conclusions

A complete geothermal system mainly comprises of heat sources, fractures and the capping. In many areas, heat source is easily identified but the major task is usually to identify the permeability controls. To achieve this, gravity structural models were developed and interpreted. Permeability is represented by fractures which form conduits for fluid flow. Compact zones are mainly represented by gravity high denoting limited or no permeability; however gravity high could also be used to denote molten magmatic material. Fractures permit movement of fluids, and heat transfer by convection nearer to the surface where they can be tapped.

The first objective of this study was to develop highly reliable gravity structural models which can be used jointly with other exploration tools to develop conceptual models. In Menengai, gravity data was modelled and an analysis of this data done by construction of Bouguer, residual gravity anomaly maps, band pass, horizontal derivative filter applications, and 3D visualisation of residual map. This objective was therefore achieved and these structural models can be seen in Chapter 4 of this report.

The second objective of this report was to establish whether there is permeability in Menengai geothermal field, Kenya. This study identified four main permeability controls for Menengai, these are: The axis of the caldera, Molo TVA, Solai TVA, Southern fault extending towards Lake Nakuru and the magmatic intrusion in the central part of the caldera. The caldera axis faults, Southern fault and the TVA's are conduits that facilitate fluid flow and therefore convective heat transfer while the magmatic intrusion was identified a permeability control due to tensional and compressional forces that would result from intruding magma.

These forces are expected to have an impact on the host rocks creating new fractures. The fractures are seen to the depth of 3 km and this information is corroborated by the drilled wells e.g. MW-01 A where the production zone has been confirmed to be between 1500 m to 3000 m. From these interpretations of the Bouguer and filtered maps, it was therefore concluded that Menengai has permeability based on the well-developed fracture networks. The indication of good permeability and the presence of a possible heat source is therefore a good encouragement for continued geothermal resources exploitation in Menengai.

The final objective was to compare gravity structural models with existing resistivity models. This was achieved by making a comparison of Horizontal derivative and resistivity models and also in terms of their operation and handling during data acquisition (Figure 22). From the models comparison, gravity came out superior since more structures were identified namely; rim of the caldera, Molo TVA and a fault structure to the south while resistivity model at the same depth only identified a magmatic intrusion in the middle of the caldera. Gravity method was also proved to be more reliable since it takes less time to take readings i.e. three (3) minutes per sampling station while MT takes twenty one (21) hours to sample one station. From these comparisons, gravity method was found to be more reliable in permeability identification and cheap to operate since it requires small workforce and is time sensitive compared to resistivity method.

In summary, good gravity models were developed by subjecting data to all necessary procedures and applying important filters for better interpretation. Permeability controls for Menengai geothermal field were identified as follows: The uplifting dome, regional fractures i.e. Solai TVA and Molo TVA, southern fault extending towards Lake Nakuru and the axis of the caldera. This has led to a conclusion that there is enough permeability in Menengai geothermal field.

5.3 Recommendations

It is recommended that more studies be done on this subject to minimise any possible chances of failure in future. This research has made a contribution to practice where it has been found to locate permeability controls that have been an elusive component using other geophysical methods e.g. resistivity. This research therefore informs the decision

makers to adopt gravity method in structure identification whenever undertaking surface exploration.

REFERENCES

Berktold, A. (1983). Electromagnetic studies in geothermal regions. *Geophysical surveys, 6*(1-2), 173-200.

Blakely, R. J. (1996). Potential theory in gravity and magnetic applications. *Cambridge University Press.*

Bonvalot, S., Diament, M., & Gabalda, G. (1998). Continuous gravity recording with Scintrex CG-3M meters: a promising tool for monitoring active zones. Geophysical Journal International, 135(2), 470-494.

Bosworth, W., Lambiase, J., & Keisler, R. (1986). A new look at Gregory's Rift: the structural style of continental rifting. *Eos, Transactions American Geophysical Union, 67*(29), 577-583.

Burke, K. and Dewey, J.F. (1973).Plume generated triple junctions: Key indicators in applying platetectonics to old rocks. J. Geol., 81: 406-433.

Einarsson, P. (1978). S-wave shadows in the Krafla caldera in NE-Iceland, evidence for a magma chamber in the crust. Bulletin of Volcanology 41(3): 187-195.

Geotermica Italiana srl, Navarro, J.M. (1987). Geothermal Reconnaissance Survey in the Menengai-Bogoria Area of the Kenya Rift Valley. 2 –Geo-volcanology. Geotermica Italiana unpublished. Final Report. TCD CON 7/85 KEN82/002. United Nations (D.T.C.D.), Republic of Kenya (M.O.E.R.D.), Pisa, Italy.

Gichira, J.M., 2012: Joint 1D inversion of MT and TEM data from Menengai geothermal field, Kenya. UNU-GTP, Iceland, report 11. 137-167.

Hasanah, L., Aminudin, A., Ardi, N. D., Utomo, A. S., Yuwono, H., Wardhana, D. D., Gaol, K.L., & Iryanti, M. (2016). Graben Structure Identification Using Gravity Method. Paper presented at the IOP Conference Series: Earth and Environmental Science (Vol. 29, No. 1, p. 012013). IOP Publishing.

Heap, M. J., Reuschlé, T., Farquharson, J. I., & Baud, P. (2018). Permeability of volcanic rocks to gas and water. Journal of Volcanology and Geothermal Research, 354, 29-38.

Hearly, J. (1975).Geothermal field zones of recent volcanism." Proceedings at the 2nd UN symposium on Development and use of geothermal resources. San Francisco, California, 1: PP 415-422.

Hinze, W. J. (1990). The role of gravity and magnetic methods in engineering and environmental studies. Geotechnical and environmental geophysics, 1, 75-126.

Jones, W.B. and Lippard, S.J. (1979).New age determination and Geology of Kenya rift-Kavirondo rift junction, west Kenya. Journ of Geol. Soc. Lon vol 136, 63pp, 693-704pp.

Khan, M.A. and Swain, C.J. (1977a). Geophysical investigations and the rift valley geology of Kenya. In:w.w.Bishop (Editor), Geological background to fossil man, Geol.soc.London, spec.publ, 6, PP 71-83.

LaFehr, T. R. (1991). Standardization in gravity reduction. Geophysics, 56(8), 1170-1178.

Leat, P.T. (1983). The structural and geochemical evolution of Menengai caldera volcano, Kenya Rift Valley. PhD thesis, University of Lancaster U.K.

Leat, P.T. (1991).Volcanological development of the Nakuru area of the Kenya rift valley. Journal of African Earth Sciences 13, 483-498.

Lee Lerner, K., Lerner, B. W., & Cengage, G. (2006). Porosity and permeability. World of Earth Science, webpage: www. enotes. com/earth-science.

Lowrie, W. (1997). Fundamentals of Geophysics. Fundamentals of Geophysics, by William Lowrie, pp. 368. ISBN 0521467284. Cambridge, UK: Cambridge University Press, October 1997., 368.

Mariita, N. O., Otieno, C.O. and Shako, J. W. (2004). Gravity studies of Menengai geothermal prospect, Kenya. Kengen Internal Report. 15 p.

Mechie, J., Prodehl, C., Ritter, J., Keller, G.R., Khan, M.A., Jacob, B., Fuchs, K., Nyambok, I. O and Obel J. D. (1997). The KRISP 94 Lithospheric investigation of southern Kenya. Tectonophysics 278, 121- 148.

Meissner, R., & Strehlau, J. (1982). Limits of stresses in continental crusts and their relation to the depthâ□frequency distribution of shallow earthquakes. Tectonics, 1(1), 73-89.

Mungania, J and Lagat, J.K. (2004). Menengai volcano: investigations for its geothermal potential a geothermal resource assessment project, Kengen internal report.

Omenda, P. A. (2007). Status of geothermal exploration in Kenya and future plans for its development. Short Course II on Surface Exploration for Geothermal Resources. UNU-GTP and Kengen, at Lake Naivasha, Kenya: 2-17.

Reynolds, J.M. (1997). An introduction to applied and environmental geophysics. John Wiley and Sons, NY, 806 pp.

Robinson, H. (2015. Conceptual hydrogeological model for caldera-associated high-enthalpy geothermal reservoirs in eastern Africa. PhD thesis, unpublished.

Schön, J. H. (2015). Physical properties of rocks: Fundamentals and principles of petrophysics (Vol. 65). Elsevier.

Searle, R.C.(1970). Evidence from gravity anomalies for the thinning of the lithosphere beneath the Rift valley in Kenya. Geophysical Journal.21: pp. 13-31.

Sentosa, R. A., Syabi, H. F., Ramadhan, A. G., & CSSSA, B. Y. (2018). Mercury and Soil Carbon Dioxide Analysis to Determine Geothermal Potential in Mt. Telomoyo, Central Java, Indonesia. ASEG Extended Abstracts, 2018(1), 1-4.

Simiyu, S. M. (1999). Induced micro-seismicity during well discharge: OW-719, Olkaria, Kenya rift. Geothermics, 28(6), 785-802.

Simiyu, S.M. (2009). Application of micro seismics methods to geothermal exploration: Examples from Kenyan rift. Presentation at Short Course V on Exploration for Geothermal Resources, UNU-GTP, GDC and Kengen, Lake Bogoria and Naivasha, Kenya, 27 pp.

Simiyu, S.M., & Keller, G.R. (1997). An integrated analysis of lithospheric structure across the East African plateau based on gravity anomalies and recent seismic studies. Tectonophysics 278, 291-313.

Simiyu, S. M., & Keller, G. R. (1998). Upper crustal structure in the vicinity of Lake Magadi in the Kenya Rift Valley region. Journal of African earth sciences, 27(3-4), 359-371.

Simiyu, S.M., & Keller, G.R. (2001). An integrated geophysical analysis of the upper crust of the southern Kenya rift. Geophysical Journal International 147, 543-561.

Smith, M. C. (1983). A history of hot dry rock geothermal energy systems. Journal of Volcanology and Geothermal Research, 15(1-3), 1-20.

Stroujkova, A. F., & Malin, P. E. (2000). A magma mass beneath Casa Diablo? Further evidence from reflected seismic waves. Bulletin of the Seismological Society of America, 90(2), 500-511.

Swain, C.J., Maguire, P.K.H., Khan, M.A. (1994). Geophysical experiments and models of the Kenya rift before 1989. Tectonophysics 236, 23-32.

Wamalwa, A.M. (2011). Joint geophysical data analysis for geothermal energy exploration. PhD thesis. University of Texas at El Paso, El Paso, Texas.

Wamalwa, A.M., Mickus, K.L., Serpa, L.F. (2013). Geophysical characterization of the Menengai volcano, Central Kenya Rift from the analysis of Magnetotellurics and gravity data. Geophysics 78, B187-B199.

APPENDIX- A section of bouguer data used in this research

Eastings	Northings	Elevation	SBA
156700	9982130	1843	-1819
156700	9983380	1824	-1813
156750	9998600	1655	-1680
156930	9979050	1914	-1837
156930	9988930	1719	-1714
156950	9987500	1737	-1752
156960	9977710	1937	-1861
157050	9973530	2035	-1888
157050	9984610	1800	-1797
157050	9991730	1679	-1733
157130	9980280	1880	-1846
157150	9983250	1821	-1814
157180	9981990	1846	-1816
157200	9982500	1836	-1812
157200	9990000	1700	-1702
157250	9999430	1681	-1664
157250	10008500	1582	-1582
157300	9992150	1674	-1727
157350	9983000	1825	-1815
157380	9978800	1919	-1844
157400	9987180	1742	-1751
157410	9977490	1945	-1868
157530	9984780	1792	-1800
157610	9989770	1698	-1718
157630	9980150	1889	-1835
157650	9992500	1659	-1734
157670	9981840	1848	-1812
157800	9986900	1746	-1754
157800	9991700	1661	-1709
157850	9978650	1926	-1834
157850	10000350	1678	-1664
157850	10006950	1574	-1603
157860	9977260	1953	-1874
157920	9989550	1699	-1726
158000	9984950	1784	-1793
158000	9992830	1658	-1706
158100	9980000	1891	-1833
158150	9981700	1853	-1813
158200	9986600	1773	-1762
158250	9984500	1787	-1803

Eastings	Northings	Elevation	SBA
170590	9998680	1614	-1658
170610	9999300	1594	-1659
170620	9999150	1596	-1664
170630	9997100	1680	-1660
170650	9974350	2010	-1794
170680	9985950	1746	-1598
170680	9997590	1673	-1654
170685	9975467	2032	-1773
170710	9997710	1665	-1655
170720	9985360	1775	-1583
170720	9997980	1639	-1660
170730	9986270	1743	-1602
170730	9992630	1648	-1663
170750	9980300	2019	-1706
170750	9997960	1640	-1660
170750	9998360	1634	-1661
170760	9997900	1643	-1653
170770	9998490	1630	-1661
170800	9982090	1993	-1658
170800	10003600	1668	-1628
170817	9973713	2031	-1756
170822	9978143	1955	-1761
170830	9986750	1723	-1604
170840	9982590	1962	-1632
170845	9974950	2036	-1768
170870	9984920	1810	-1585
170900	9974600	2030	-1794
170930	9972500	2130	-1696
170930	9983470	1893	-1616
170930	9987250	1714	-1603
170945	9972706	2015	-1777
170950	9988520	1724	-1633
170972	9973346	2035	-1777
170980	9994400	1652	-1644
170988	9979704	1960	-1791
171030	9982030	2004	-1655
171030	9987750	1711	-1612
171050	9987130	1711	-1607
171050	9996850	1680	-1662
171070	9982180	2001	-1660

158250	10012100	1576	-1558
158270	9977050	1960	-1873
158300	9978450	1934	-1835
158300	9993230	1652	-1692
158350	9985310	1777	-1784
158400	10001150	1681	-1659
158400	10005550	1572	-1613
158430	9989360	1701	-1728
158480	9977510	1952	-1865
158550	9973280	2051	-1886
158600	9979850	1897	-1825
158600	9986350	1746	-1766
158600	9993230	1643	-1685
158630	9981550	1857	-1810
158640	9985580	1772	-1779
158650	9984180	1796	-1800
158680	9977970	1942	-1852
158730	9976840	1967	-1915
158750	10003950	1581	-1620
158780	9989110	1703	-1723
158800	10013150	1571	-1542
158830	9989610	1689	-1717
158880	9978440	1930	-1841
158880	9988650	1711	-1730
158900	9994030	1635	-1685
158910	9990110	1682	-1717
158950	9990500	1678	-1713
158960	9985740	1766	-1772
159000	9972120	2074	-1893
159050	9983900	1795	-1801
159090	9978890	1920	-1831
159110	9981410	1865	-1809
159120	9988150	1715	-1734
159150	9991000	1672	-1717
159180	9976620	1974	-1892
159180	9994450	1632	-1674
159200	10001400	1590	-1616
159220	9986160	1762	-1764
159280	9991480	1661	-1723
159300	9979360	1910	-1823
159330	9987640	1722	-1745
159440	9987150	1737	-1749
159460	9991950	1655	-1729
159480	9983600	1801	-1806

171080	9990740	1646	-1633
171100	9968600	1845	-1800
171100	9980650	2037	-1689
171111	9975500	2038	-1781
171127	9978696	1950	-1746
171130	9988230	1715	-1626
171170	9983830	1867	-1612
171170	9984490	1838	-1599
171180	9982950	1936	-1626
171187	9973741	2056	-1740
171200	9992480	1649	-1669
171235	9973942	2036	-1755
171250	9986450	1736	-1594
171250	9988750	1735	-1637
171262	9975391	2070	-1774
171270	9973258	2037	-1748
171333	9973499	2072	-1750
171350	9990810	1650	-1673
171350	9974560	2025	-1792
171400	9989880	1699	-1658
171409	9972689	2009	-1782
171430	9972500	2015	-1685
171440	9982290	1986	-1664
171450	9988510	1717	-1643
171473	9973969	2056	-1774
171478	9980099	1944	-1789
171480	9981800	2010	-1650
171490	9990720	1655	-1672
171495	9975625	2074	-1784
171500	9987080	1712	-1606
171520	9990980	1652	-1677
171550	9990870	1656	-1677
171550	9974450	2043	-1785
171566	9973283	2069	-1742
171580	9980700	2028	-1670
171606	9975455	2072	-1773
171610	9974683	2067	-1759
171620	9984150	1844	-1618
171640	9994350	1657	-1655
171711	9975114	2084	-1750
171712	9980325	1930	-1812
171734	9972872	2042	-1781
171750	9986450	1737	-1606
171750	9989530	1687	-1658

159500	9973150	2062	-1875
159500	9994830	1628	-1659
159510	9979810	1902	-1815
159520	9986720	1750	-1743
159590	9981270	1869	-1802
159610	9986440	1759	-1740
159620	9976380	1981	-1864
159640	9992420	1650	-1712
159700	9980270	1894	-1812
159710	9985950	1768	-1748
159780	9995200	1622	-1655
159810	9984370	1847	-1802
159810	9985460	1778	-1761
159820	9992880	1644	-1695
159850	9978880	1948	-1840
159870	9986540	1755	-1722
159900	9983330	1818	-1794
159900	10013600	1519	-1547
159960	9980240	1884	-1802
159970	9984990	1789	-1774
160010	9993350	1637	-1681
160030	9993490	1632	-1672
160070	9976150	1989	-1839
160080	9995630	1614	-1651
160090	9981120	1878	-1801
160100	9974480	2037	-1871
160150	9991400	1662	-1691
160210	9986820	1749	-1733
160220	9993810	1627	-1664
160230	9984570	1799	-1781
160250	9993310	1634	-1676
160300	9978750	1933	-1819
160300	9983080	1835	-1789
160300	10001500	1567	-1608
160300	10014100	1475	-1549
160330	9977750	1952	-1839
160350	9996030	1607	-1643
160410	9984370	1803	-1781
160430	9978070	1944	-1834
160500	9973000	2069	-1863
160500	9991000	1659	-1681
160500	9993100	1634	-1675
160500	9994240	1620	-1660
160510	9975910	1997	-1810
171750	9993300	1645	-1686
171750	9993800	1646	-1681
171750	9994800	1654	-1687
171761	9979937	1916	-1740
171764	9974477	2071	-1772
171780	9995300	1661	-1683
171800	9996350	1691	-1693
171856	9973496	2066	-1740
171861	9974066	2079	-1798
171870	9988520	1708	-1647
171880	9972530	2125	-1677
171880	9990340	1667	-1669
171880	9995800	1672	-1671
171900	9981550	2006	-1666
171900	9991310	1652	-1675
171900	10002800	1784	-1644
171910	9983870	1848	-1627
171912	9973054	2035	-1798
171914	9980286	1890	-1807
171927	9973040	2049	-1765
171930	9982290	1980	-1661
171934	9975605	2090	-1780
171936	9974717	2075	-1777
171940	9973242	2051	-1771
171950	9980850	2028	-1684
171953	9975661	2090	-1735
171981	9979310	1958	-1746
171987	9973646	2066	-1779
172000	9987030	1718	-1603
172000	9975850	2090	-1783
172021	9974651	2078	-1814
172031	9975610	2095	-1770
172040	9984370	1811	-1619
172058	9976613	2103	-1731
172070	9994220	1660	-1658
172079	9975872	2105	-1791
172080	9974038	2080	-1747
172100	9996730	1716	-1704
172130	9981200	1998	-1685
172130	9989960	1673	-1661
172130	9996250	1686	-1693
172133	9972854	2040	-1800
172150	9990050	1665	-1676
172150	9995750	1692	-1664

160540	9987200	1741	-1722
160560	9984190	1808	-1779
160580	9979100	1926	-1816
160590	9984570	1801	-1777
160650	9978400	1937	-1825
160680	9996450	1602	-1629
160700	9978050	1949	-1824
160700	9984730	1794	-1774
160700	10016250	1462	-1536
160730	9982750	1841	-1801
160730	9987400	1738	-1716
160830	9975640	2001	-1847
160850	9978750	1937	-1819
160850	9994630	1614	-1657
160860	9992810	1631	-1673
160890	9983810	1818	-1780
160900	9990700	1656	-1665
160900	9996830	1596	-1629
160950	10014850	1452	-1543
160960	9984960	1794	-1776
161030	9976320	1990	-1835
161040	9987450	1735	-1707
161100	9977750	1960	-1821
161140	9975630	2005	-1839
161200	9997300	1586	-1628
161200	10015100	1452	-1542
161220	9983430	1833	-1781
161250	9976760	1983	-1822
161250	9994930	1608	-1648
161260	9992510	1626	-1666
161280	9990750	1664	-1660
161290	9987900	1734	-1697
161300	9985330	1792	-1753
161380	9994550	1620	-1645
161400	9985420	1787	-1750
161440	9988290	1739	-1692
161470	9992340	1628	-1666
161500	10000600	1567	-1610
161520	9983030	1848	-1782
161530	9977250	1976	-1813
161530	9995350	1606	-1640
161550	9976380	1997	-1817
161630	9975540	2012	-1825
161640	9985680	1788	-1744
172170	9971280	1997	-1673
172170	9971750	2045	-1673
172170	9972200	2105	-1673
172180	9995250	1668	-1682
172200	9986550	1741	-1612
172200	9994730	1665	-1668
172203	9980365	1855	-1848
172208	9977207	2100	-1748
172210	9989490	1684	-1658
172220	9985940	1767	-1684
172230	9990450	1657	-1679
172240	9984970	1782	-1598
172250	9970750	1949	-1670
172250	9970750	1949	-1670
172250	9985290	1766	-1599
172250	9990850	1650	-1687
172254	9977908	2089	-1761
172270	9988400	1710	-1648
172270	9991660	1654	-1683
172277	9978591	2026	-1753
172283	9976113	2125	-1746
172287	9974696	2072	-1785
172290	9994240	1660	-1661
172300	9970250	1908	-1681
172300	9970250	1908	-1681
172300	9993830	1658	-1665
172300	10003100	1795	-1648
172310	9993550	1657	-1668
172320	9985870	1746	-1606
172320	9989390	1679	-1660
172336	9981863	1950	-1880
172350	9969800	1890	-1675
172350	9969800	1890	-1675
172354	9981624	1990	-1857
172358	9976454	2119	-1737
172370	9986390	1733	-1612
172397	9975778	2128	-1722
172400	9969330	1871	-1671
172400	9969330	1871	-1671
172400	9982490	1956	-1651
172400	9991230	1650	-1693
172420	9994600	1662	-1668
172430	9986890	1722	-1612
172440	9983700	1837	-1633

161670	9977540	1972	-1809
161680	9992020	1629	-1661
161700	9990780	1680	-1654
161700	10014700	1456	-1540
161710	9988660	1738	-1670
161750	9994200	1619	-1642
161760	9985820	1787	-1740
161760	9995790	1603	-1628
161780	9996310	1596	-1630
161800	9988050	1763	-1710
161800	10012750	1474	-1547
161820	9982630	1863	-1778
161850	9986500	1775	-1734
161850	9987000	1765	-1710
161850	9987550	1772	-1705
161850	9988500	1754	-1672
161850	10009900	1502	-1568
161850	10011200	1498	-1565
161880	9996740	1588	-1636
161940	9997480	1568	-1627
161950	9976100	2005	-1814
161950	9999200	1568	-1621
161970	9988830	1732	-1662
161970	9997080	1581	-1631
162030	9986000	1778	-1731
162030	9991860	1637	-1655
162050	9986100	1773	-1727
162100	9972700	2083	-1820
162110	9982220	1877	-1777
162120	9975450	2020	-1811
162130	9993900	1619	-1640
162140	9988850	1731	-1656
162140	9988850	1731	-1656
162180	9987350	1741	-1692
162180	9990800	1712	-1647
162190	9977550	1975	-1803
162190	9985440	1788	-1734
162240	9997770	1556	-1623
162280	9977660	1977	-1803
162290	9981980	1884	-1778
162290	9985620	1783	-1726
162320	9988740	1727	-1661
162320	9988740	1727	-1661
162350	9975800	2016	-1812

172450	9996450	1690	-1703
172456	9981104	1841	-1753
172460	9989250	1680	-1661
172480	9987380	1712	-1637
172480	9992600	1659	-1677
172490	9980566	1850	-1828
172520	9987830	1708	-1651
172530	9997500	1701	-1717
172547	9972256	2048	-1795
172550	9997000	1696	-1712
172559	9980858	1761	-1817
172576	9973505	2068	-1767
172590	9988360	1708	-1656
172590	9995160	1664	-1676
172600	9996150	1674	-1704
172650	9991990	1657	-1684
172700	9991650	1652	-1682
172700	9993170	1656	-1679
172730	9982860	1905	-1646
172730	9989700	1661	-1691
172750	9991850	1649	-1694
172757	9972671	2058	-1783
172766	9980673	1840	-1817
172790	9995780	1675	-1684
172800	9990200	1664	-1679
172800	9990650	1663	-1683
172830	9985790	1746	-1620
172840	9988920	1694	-1666
172880	9983560	1845	-1636
172880	9991150	1658	-1695
172880	9974652	2060	-1795
172889	9976440	2142	-1736
172901	9981878	1985	-1804
172921	9980243	1828	-1878
172950	9995250	1660	-1706
172950	9996280	1690	-1681
172960	10000030	1752	-1679
172970	9991670	1660	-1693
172970	9980903	1800	-1854
173000	9968650	1844	-1691
173006	9973425	2075	-1768
173030	9992330	1661	-1693
173030	9996570	1701	-1686
173051	9980543	1790	-1796

162380	9977630	1975	-1801
162380	9985160	1787	-1733
162410	9981820	1888	-1777
162420	9986500	1774	-1634
162470	9981780	1889	-1775
162500	9993550	1619	-1628
162500	10008200	1514	-1586
162540	9988570	1721	-1655
162540	9988570	1721	-1655
162550	9987750	1727	-1658
162580	9975350	2026	-1798
162620	9991600	1657	-1637
162640	9984860	1793	-1732
162670	9989000	1720	-1631
162670	9989000	1720	-1631
162670	9997370	1577	-1620
162700	9990650	1712	-1624
162700	10005400	1530	-1600
162710	9982180	1887	-1770
162720	9992140	1627	-1664
162730	9981440	1899	-1772
162730	9986830	1732	-1673
162750	9975370	2025	-1801
162750	9975500	2016	-1810
162800	10006250	1526	-1594
162850	9989630	1719	-1616
162850	9989630	1719	-1616
162870	9984530	1803	-1703
162880	9988130	1717	-1637
162940	9989940	1717	-1607
162940	9989940	1717	-1607
162980	9993450	1622	-1628
162990	9991430	1679	-1643
163000	9975930	2009	-1802
163000	9999100	1557	-1613
163010	9990200	1713	-1605
163010	9990200	1713	-1605
163050	9981060	1914	-1773
163050	9982650	1884	-1770
163050	9987150	1825	-1662
163090	9997000	1574	-1619
163100	9991380	1681	-1638
163110	9990530	1708	-1602
163110	9990530	1708	-1602
173063	9972757	2062	-1766
173070	9988680	1695	-1669
173080	9992990	1657	-1697
173086	9979846	1920	-1791
173110	9983000	1869	-1652
173120	9988400	1705	-1669
173120	9988560	1704	-1671
173130	9994750	1652	-1699
173150	9996900	1708	-1674
173153	9974624	2090	-1801
173161	9981623	1919	-1813
173200	9996030	1673	-1689
173249	9976276	2164	-1738
173260	9988380	1702	-1670
173278	9980956	1826	-1781
173290	9997370	1699	-1685
173300	9994300	1647	-1718
173330	9983380	1856	-1657
173348	9972759	2053	-1787
173360	9985100	1775	-1635
173364	9979254	1954	-1801
173380	9992500	1661	-1693
173390	9985800	1752	-1649
173391	9974071	2049	-1814
173391	9974071	2049	-1814
173430	9985510	1762	-1648
173440	9997830	1706	-1699
173470	10004400	1722	-1659
173500	9988950	1692	-1682
173500	9993830	1650	-1721
173530	9992250	1663	-1704
173550	9989450	1685	-1684
173550	9995580	1665	-1724
173570	9987900	1710	-1669
173580	10000060	1737	-1688
173590	9998300	1715	-1708
173600	9989930	1681	-1684
173601	9973187	2063	-1807
173620	9983240	1867	-1670
173650	9990450	1670	-1704
173650	9990850	1667	-1711
173680	9996200	1683	-1689
173700	9991300	1665	-1715
173700	9991780	1666	-1715

163130	9980920	1919	-1773
163140	9984290	1797	-1722
163160	9980310	1930	-1765
163170	9977600	1980	-1797
163230	9985350	1772	-1654
163240	9975250	2025	-1795
163250	9976380	2002	-1800
163250	9987950	1719	-1628
163260	9980540	1830	-1773
163260	9996400	1578	-1615
163300	9982460	1892	-1766
163300	9987500	1724	-1640
163350	10004000	1534	-1617
163410	9980060	1937	-1772
163430	9980060	1936	-1771
163450	9976830	1996	-1801
163450	9982350	1894	-1763
163450	9991230	1668	-1636
163450	9993400	1623	-1630
163450	10007500	1529	-1577
163480	9977280	1989	-1801
163490	9995960	1584	-1614
163500	10000700	1547	-1633
163510	9990330	1702	-1609
163510	9990330	1702	-1609
163600	9987800	1723	-1625
163600	10002300	1540	-1633
163650	9991120	1670	-1629
163670	9977530	1985	-1793
163670	9982170	1897	-1760
163680	9979610	1944	-1776
163720	9995500	1593	-1610
163740	9975160	2027	-1788
163750	9975500	2028	-1783
163800	9984100	1788	-1714
163870	9978630	1956	-1735
163880	9982000	1902	-1759
163910	9980710	1924	-1762
163910	9991020	1671	-1620
163930	9993500	1621	-1619
163940	9979190	1954	-1775
163950	9979270	1952	-1775
163950	9995020	1602	-1616
164000	9975950	2020	-1782

173700	9993350	1655	-1716
173704	9974528	2055	-1809
173730	9998760	1715	-1705
173762	9979001	1945	-1803
173780	9995230	1666	-1722
173782	9978729	1990	-1806
173790	9986000	1750	-1668
173840	9987590	1726	-1672
173851	9973091	2060	-1794
173876	9973565	2043	-1819
173920	9999320	1718	-1702
173980	9987410	1734	-1676
173991	9976305	2123	-1786
174000	9999600	1722	-1698
174020	9981387	1824	-1781
174030	9987430	1734	-1677
174050	9992160	1667	-1719
174050	9996430	1682	-1707
174060	9983310	1853	-1675
174074	9982102	1827	-1797
174080	9987780	1728	-1672
174090	9988300	1709	-1691
174090	9999870	1725	-1694
174092	9982288	1907	-1875
174100	9994730	1668	-1731
174110	9988130	1720	-1687
174122	9974680	2060	-1724
174122	9975980	2096	-1741
174130	9988770	1700	-1696
174151	9974188	2072	-1728
174156	9973351	2055	-1789
174160	9989530	1689	-1707
174160	9989530	1689	-1714
174170	9989250	1695	-1699
174171	9980701	1826	-1778
174171	9973755	2065	-1739
174200	9987110	1746	-1682
174200	9989920	1689	-1706
174200	10005270	1667	-1677
174226	9975092	2054	-1745
174230	9990810	1685	-1725
174250	9991030	1682	-1726
174265	9978554	1963	-1786
174360	9991550	1676	-1729

164050	9988840	1706	-1594
164050	9990040	1698	-1601
164050	9990400	1698	-1601
164080	9994500	1610	-1618
164090	9975070	2032	-1785
164130	9996100	1575	-1620
164130	9996500	1575	-1606
164150	9979470	1949	-1771
164150	9983920	1790	-1717
164160	9977470	1991	-1787
164220	9994020	1613	-1614
164230	9978770	1965	-1773
164230	9981140	1921	-1757
164230	9997400	1559	-1621
164230	9997400	1559	-1621
164250	9976400	2012	-1787
164280	9993800	1615	-1613
164300	9981720	1914	-1757
164300	9993600	1620	-1613
164330	9978800	1963	-1774
164340	9980840	1670	-1613
164340	9984150	1782	-1711
164350	9993530	1618	-1618
164360	9974960	2031	-1776
164430	9989820	1674	-1639
164430	9989820	1674	-1639
164430	9995750	1590	-1613
164450	9972000	2088	-1790
164460	9984300	1781	-1701
164480	9979770	1947	-1768
164480	9993050	1626	-1617
164500	9992860	1629	-1618
164500	9997400	1557	-1618
164500	9997850	1557	-1618
164530	9981540	1918	-1751
164580	9978410	1979	-1770
164600	9976050	2018	-1777
164600	9983500	1807	-1714
164600	9983500	1807	-1714
164610	9977790	1992	-1773
164640	9984540	1780	-1690
164650	9992290	1638	-1613
164670	9974760	2031	-1777
164770	9989400	1693	-1613

174371	9975314	2067	-1707
174400	9992080	1671	-1740
174407	9975687	2087	-1672
174420	9985780	1784	-1685
174420	9991840	1674	-1738
174444	9973355	2150	-1751
174450	9993900	1660	-1742
174450	9994350	1667	-1741
174460	9986750	1759	-1681
174490	9983560	1845	-1675
174530	9996600	1677	-1725
174550	9999680	1716	-1708
174600	9968900	1849	-1674
174600	9995430	1684	-1727
174640	9995900	1690	-1720
174654	9980180	1840	-1801
174690	9986420	1772	-1693
174700	9968300	1863	-1664
174730	9994450	1679	-1720
174730	9994930	1685	-1718
174750	9996400	1694	-1719
174750	10003800	1654	-1691
174813	9973427	2190	-1779
174830	9996930	1689	-1726
174925	9978014	1906	-1805
174960	9983570	1854	-1688
174980	9999520	1720	-1710
175050	9985850	1787	-1706
175050	9997350	1699	-1731
175146	9980274	1837	-1789
175150	9994000	1670	-1744
175220	9999430	1734	-1719
175298	9974179	1985	-1824
175303	9976814	2009	-1788
175370	9997750	1713	-1742
175371	9980625	1831	-1799
175411	9978240	1890	-1770
175438	9970492	2020	-1769
175460	9983520	1861	-1701
175491	9972995	2270	-1830
175500	10002500	1623	-1731
175510	9999310	1712	-1730
175530	9984480	1839	-1707
175530	9985730	1799	-1719

164770	9990640	1668	-1606
164770	9991820	1649	-1619
164780	9978400	1969	-1774
164800	9993700	1616	-1615
164800	9993700	1616	-1615
164800	10007950	1550	-1576
164820	9989970	1680	-1610
164840	9989460	1692	-1605
164840	9990360	1672	-1609
164860	9990620	1667	-1604
164870	9990650	1666	-1601
164900	9978060	1987	-1769
164900	9980150	1943	-1760
164900	9983900	1797	-1691
164900	9983900	1797	-1691
164900	9991330	1655	-1604
164950	9975700	2023	-1774
164950	9984940	1776	-1674
165000	9990940	1662	-1596
165030	9992380	1633	-1626
165030	9992380	1633	-1626
165050	9988860	1708	-1598
165070	9980320	1941	-1755
165100	9983480	1807	-1713
165100	9983480	1807	-1713
165200	9969900	1919	-1660
165200	9978650	1965	-1777
165200	9984300	1791	-1678
165200	9984300	1791	-1678
165200	9991180	1654	-1602
165200	9991180	1654	-1602
165220	9989790	1697	-1582
165230	9983100	1823	-1723
165230	9983100	1823	-1723
165250	9974110	2029	-1767
165260	9977700	1992	-1766
165280	9988510	1721	-1583
165280	9993800	1615	-1613
165300	9975300	2025	-1770
165390	9980630	1941	-1745
165410	9988410	1724	-1581
165480	9984700	1791	-1653
175530	9974456	1985	-1855
175540	9983960	1850	-1703
175550	9985260	1813	-1714
175550	9990730	1716	-1732
175550	9991180	1715	-1741
175577	9981080	1836	-1799
175580	9991630	1712	-1750
175580	9993180	1681	-1777
175600	9970900	2012	-1674
175600	9992150	1692	-1771
175600	9992600	1682	-1769
175600	9993600	1680	-1776
175600	9994080	1667	-1771
175600	9994780	1677	-1761
175600	9995280	1676	-1739
175610	9984830	1832	-1712
175633	9970889	2075	-1760
175650	9998150	1729	-1746
175720	9986320	1792	-1727
175726	9974805	1968	-1811
175740	9999230	1701	-1729
175770	9986690	1787	-1732
175790	9988360	1762	-1742
175800	9995780	1663	-1755
175810	9987050	1783	-1733
175810	9989110	1745	-1748
175820	9985370	1823	-1724
175830	9988920	1750	-1746
175860	9987970	1767	-1742
175860	9988650	1759	-1746
175870	9987490	1770	-1734
175880	9989590	1738	-1756
175880	9975053	1974	-1807
175886	9977809	1925	-1811
175900	9998680	1718	-1754
175902	9971337	2105	-1806
175920	9983730	1865	-1711
175931	9981556	1826	-1805
175946	9972677	2250	-1805
175950	9992200	1684	-1772
175984	9975350	1981	-1808
176010	9990140	1722	-1770